UNIVERSITY OF TWENTE.

Faculty of Engineering Technology

Tool Wear in Sheet Metal Forming

Modelling of Abrasive Tool Wear in Hot Forming

Graduation assignment at TriboForm Engineering

Name:	C.A. van der Veen
Programme:	Master Mechanical Engineering
Chair:	Nonlinear Solid Mechanics
UT supervisor:	dr. J. Hazrati Marangalou
Company:	TriboForm Engineering
External supervisors:	dr.ir. D. Waanders
	dr.ir. J. Hol

Enschede, April 11, 2024

Summary

Abrasive tool wear is a common phenomenon in hot forming operations, due to the high temperatures and lack of lubrication. Abrasive wear is the removal of material from the tool. The condition of the tool has a direct influence on the quality of the product. When severe tool wear occurs, the quality of the product becomes insufficient and the tool needs to be repaired or replaced. Therefore, it is of interest to predict the location and severity of tool wear.

The aim of this research is to develop an abrasive tool wear model for hot forming operations, so manufacturers can simulate the tool wear and predict the tool life time. Volvo Cars provided a data set with the simulation and tool scans of an A-pillar to develop this model. A sensitivity study is conducted to find a correlation between process parameters and the amount of tool wear. This resulted in a promising model. The model determines the amount of tool wear based on the dissipation of energy and has a variable wear coefficient. The nonlinear development of tool wear is incorporated in the model by relating the wear coefficient to the sliding distance.

The model is calibrated for a tribological system with a boron steel with AlSi coating and an uncoated tool steel 1.2344, which is a common system for hot forming operations. The model is validated on the lower dies of the Volvo Cars A-pillar. The validation shows that the model can successfully predict the locations where abrasive tool wear occurs. The severity of tool wear is accurate at locations which experience a significant sliding distance. In the areas with a small sliding distance the amount of tool wear is underestimated by a factor 10. An adjustment to the calibration procedure is proposed to solve this underestimation. The model can be used to predict the tool life time when an abrasive wear limit is provided.

Nomenclature

Abbreviations

AF	AutoForm
COF	Coefficient Of Friction
IWR	Instantaneous Wear Rate
SMF	Sheet Metal Forming
SSWR	System Specific Wear Rate
TF	TriboForm
TW	Tool Wear
UHSS	Ultra High Strength Steel

Greek Symbols

α	Fractional real area of contact
α_{max}	Maximum real area of contact
ϵ	Equivalent plastic strain
μ	Coefficient of Friction
ν	Sliding Velocity

Other Variables

a	Constant in wear rate k
b	Constant in wear rate k
dl	Sliding length
F_f	Frictional Force
F_N	Normal Force
H	Hardness
k	Wear Rate or Wear Coefficient
P	Pressure
T	Temperature
V	Wear Volume

Contents

1 Introduction

1.1 Sheet Metal Forming

Sheet Metal Forming (SMF) is a manufacturing process where a thin metal sheet is formed into the desired shape. Deep drawing is a SMF process which is widely used for the manufacturing of car body parts. The tools for this process consist of a die, blankholder and punch. Figure 1 shows the setup before the forming operation starts. The sheet metal, called the blank, is placed in the blankholder. The blankholder controls material flow into the die. The punch is pushed down and forces the blank into the shape of the die. This results in a product in the desired shape. However, the deep drawing process comes with some challenges. The sheet can experience splits, wrinkles, scratches and springback of the final product. Abrasive wear and galling are a common problem for the tool and may reduce product quality and efficiency of the process. Simulation of the manufacturing process is a useful tool to find a good design and suitable process settings to prevent these problems from occurring in manufacturing.

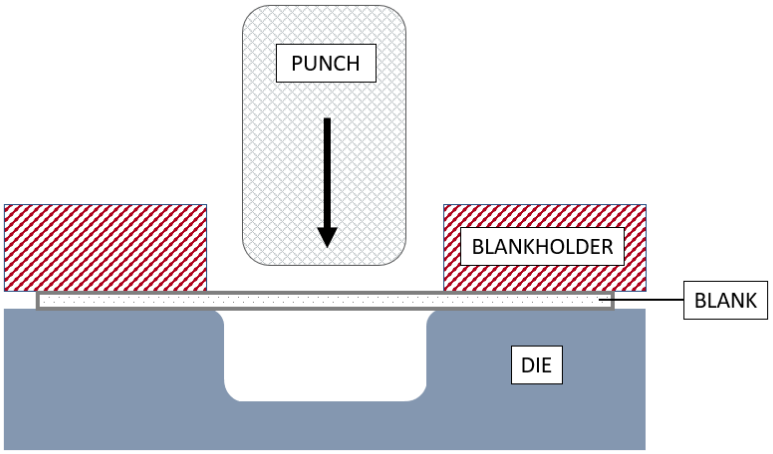

Figure 1: Schematic overview of the deep drawing process

Deep drawing can be executed as a cold forming and a hot forming process. Which one is applied depends on the desired mechanical properties of the product. Cold forming takes place at room temperature and uses a lubricant. Hot forming takes place at elevated temperatures to improve formability and mechanical properties of the product. Lubricants are seldomly used in the hot forming process, since they are not suitable for the high temperatures. Structural parts are generally produced with a hot forming process, since these parts have a higher strength requirement. This can be achieved with hot forming and quenching. However, at elevated temperatures more tool wear is experienced, which is a disadvantage of the hot forming process.

AutoForm is a company that provides software solutions for Sheet Metal Forming and Body-in-White assembly and is therefore useful for manufacturing processes in the automotive industry. The AutoForm software provides the FormingSolver, which makes it possible to simulate SMF processes.

The TriboForm Analyzer is a software programme that can simulate friction and lubrication conditions for a specific tribological system. The characteristics of the system can be exported to a TriboForm Library. This library can be used as a plug-in for the AutoForm software and improves the accuracy of SMF simulation results.

1.2 Tool Wear

After producing a certain amount of products, tools begin to show signs of wear. In SMF abrasive and adhesive wear takes place. Abrasive wear is the removal of tool material, e.g. scratches on the tool surface. Adhesive wear takes place in the form of galling, which means that small particles of the product stick to the tool. These wear mechanisms can also interact with each other.

The condition of the tool has a direct influence on the quality of the product. When severe tool wear occurs, the quality of the product becomes insufficient and the tool needs to be repaired or replaced.

Therefore, it is of interest to simulate the location and severity of tool wear. With this information the tool life can be predicted and adaptions can be made to improve tool life. In previous research a galling model for hot forming is developed [1]. Therefore, the focus of this research is abrasive tool wear in hot forming.

1.3 Objective

The objective of this research is to develop a model that describes abrasive tool wear in hot forming processes. This is done by looking for a correlation between process parameters from the simulation and the abrasive tool wear obtained from experimental data. Volvo Cars provided simulation and experimental data of an A-pillar. The A-pillar is the first vertical support in a car and is of importance for the structural integrity, since it carries the roof and protects the passengers in case of a collision. The different pillars in a car are indicated in Figure 2.

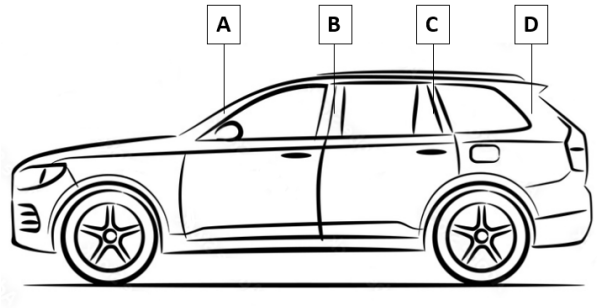

Figure 2: A-, B-, C- and D-pillar in a car

The simulation that is provided by Volvo Cars shows the manufacturing process of an A-pillar. The tools that are used for manufacturing of the A-pillar and the final product are shown in Figure 3. The final product in Figure 3b contains both the right and left A-pillar of the car, both parts are manufactured in one product.

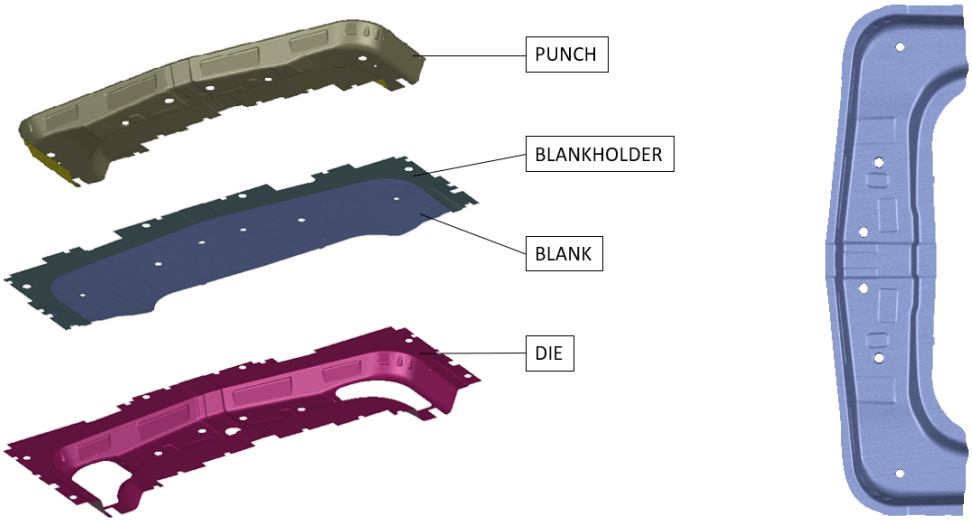

(a) Tools (b) Final product

Figure 3: Volvo Cars A-pillar

The purpose of the model is to predict tool wear, and possibly improve the tool life. The following steps are taken to conduct the research:

- Literature study

- Sensitivity study
- Definition of an abrasive tool wear model
- Calibration of the model
- Validation of the model

1.4 Outline

In this chapter the research area and objective are briefly discussed. The Literature review in Chapter 2 describes the background that is needed for the research. In Chapter 3, the Method, an overview of the research is given, as well as a step-by-step guide to conduct the research. In the Tool Wear model in Chapter 4 the data is collected and the current model is tested. Different formulations of the wear rate and different models are analysed. The most promising model is chosen as the final model. In Chapter 5, Calibration, this model is optimised to fit the experimental data with the smallest error. Once the model is calibrated, a validation case is executed in the Validation, Chapter 6. The research is completed with the Discussion, Conclusion and Recommendations in Chapter 7, 8 and 9, respectively.

2 Literature

To develop an abrasive tool wear model, it is necessary to understand the background. In this literature study tribology, wear and existing wear models are discussed. An overview of the subjects and their relation is shown in Figure 4.

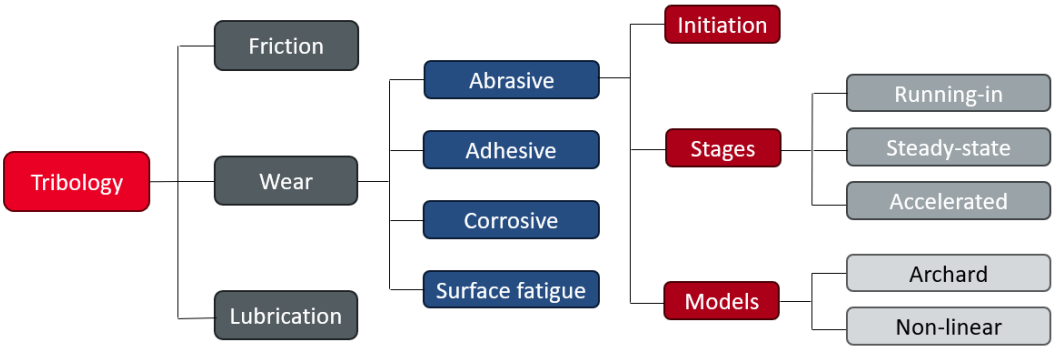

Figure 4: Literature overview

2.1 Tribology

Tribology is the study of friction, wear and lubrication for contacting surfaces that are in relative motion. Changes in either the friction, wear or lubrication influence each other and should therefore be analysed as a whole. In the deep drawing process there is sliding contact between the tool and sheet. A tribological system consists of the sheet, tool and lubricant. Before elaborating on tribology, the contact between surfaces is defined.

Contact

While some surfaces appear very smooth on macro level, every surface has a roughness when you take a closer look. This roughness consists of asperities. When two surfaces are in contact, the nominal contact area neglects the roughness of the surfaces. The real contact area does take the roughness into account. This means that only the top of the asperities that are in contact with the other surface are counted as the contact area. The real contact area increases when the surface is loaded with a normal force, this is called flattening. Flattening is assumed to be a plastic deformation. The nominal contact area, the real contact area and flattening are illustrated in Figure 5.

Friction

Friction is the resistance force between two surfaces in sliding contact. From the classical friction laws it follows that friction is independent of the area in contact and directly proportional with the normal force. Coulomb friction describes the dry friction force and is given in Equation 1. Where F_f is the force of friction, μ the Coefficient Of Friction(COF) and F_N the normal force.

$$F_f \leq \mu F_N \tag{1}$$

In many FE-simulations of forming processes, the Coulomb friction model is applied, using a constant COF. However, according to Hol [2], the friction coefficient is dependent on process parameters like the contact pressure and contact area. Since the contact pressure can result in a plastic deformation of the surface topography, the contact area can change during the forming process. This means the COF is a variable and a constant friction does not give an accurate approximation of the COF. Beside this, in many cold forming processes a lubricant is used. Therefore the Coulomb friction model, meant for dry friction, is highly inaccurate. For systems where a lubricant is applied the Stribeck curve can be used to determine the COF.

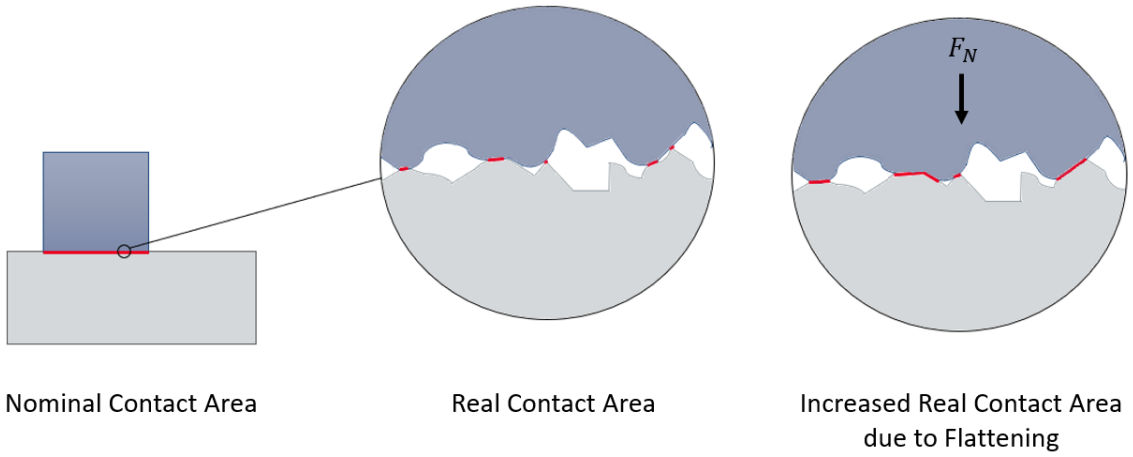

Figure 5: Contact Area

There are different test methods to experimentally determine the COF for hot forming processes. In Figure 6 the development of the friction coefficient with increasing temperature of different test methods is shown. From this and other researches follows that friction is temperature dependent, in general one can conclude that the COF decreases with increasing temperature [3, 4, 5].

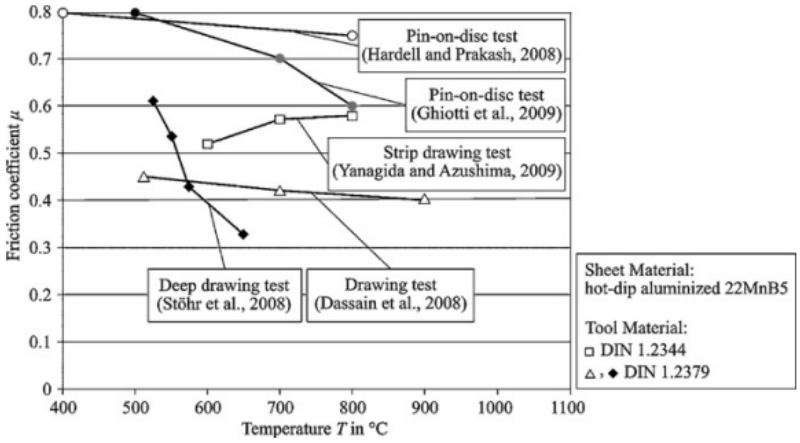

Figure 6: Friction coefficient against temperature [3]

There are several explanations for this temperature dependency. One is the development of oxidation layers and the reduced adhesion following from that, resulting in a decreasing COF [3, 4, 6]. Another possible cause is that that the elevated temperature results in an easier deformation of asperities, so the change in surface topography results in a lower COF [3, 7]. Also the increased tool wear at high temperatures can result in a change of COF [3].

To prevent oxidation and/or scale formation a coating can be applied to protect the base material during hot forming operations. An Al-Si coating is commonly used in this application [3, 4].

In the research of Venema et al. [7] subsequent strip draw tests are executed to examine the temperature dependency. After the first draw the temperature dependency decreases, probably due to the development of a tribo-layer on the tools. The Al-Si coating adheres to the tool surface, and debris is embedded into the sheet. This changes the characteristics of the tribological system, and therefore also the COF [8].

From the researches can be concluded that the COF is not a constant, and that there are many processes that can influence the COF. Coatings are used to control these processes up to a certain level.

Wear

Wear is the progressive damaging of two surfaces in contact. There are different wear mechanisms and different stages of wear, which will be discussed in Section 2.2. In deep drawing, mainly abrasive and adhesive wear are experienced. The development of oxidation layers is also observed in hot forming processes [4]. A temperature dependency is observed for tool wear. The amount of tool wear increases with increasing temperature [4, 7]. The amount of wear decreased when a Al-Si coating was applied [4]. There are cases where the wear decreases with increasing temperature, this is probably caused by the formation of a oxidation layer, which protects the tool from wear [4].

From the research of Hardell et al. [4], where friction and wear tests were conducted at 40 °C, 400 °C and 800 °C, followed that adhesive wear occurred at all temperatures, while abrasive wear and oxidation only occurred at higher temperatures. The research of Venema et al. [7] showed similar results. At temperatures above 600 °C abrasive wear took place, followed up by compaction galling. At temperatures below 600 °C mainly adhesive wear took place.

Lubrication

During cold forming, a lubricant is used in a tribological system to protect the blank and tools from wear and enhance material flow in the forming process. There are three lubrication regimes: boundary lubrication, mixed lubrication and hydrodynamic lubrication. In the boundary lubrication regime, there is minimal lubrication and the surfaces are in direct contact with each other at the top of the asperities. The lubrication is located in the valleys of the surface topography and the load is carried by the asperities. In the hydrodynamic lubrication regime, there is a full lubrication film between the surfaces, there is no direct contact between asperities. The load is entirely carried by the lubricant. Within the mixed lubrication regime the conditions are in between the boundary lubrication and the hydrodynamic lubrication regime, i.e. the load is carried by both asperities and lubricant. The Stribeck curve shows the relation between the COF and the lubrication regime. Lubricants are mainly used in cold forming processes. There are some lubricants developed specifically for hot forming, however, it is not a common practice to use a lubricant in hot forming. [9]

Material

A sheet material that is commonly used for hot forming purposes is a boron steel alloy 22MnB5, with an Al-Si coating. 22MnB5 is an ultra high strength steel (UHSS). This material is very suitable for structural parts, since a fully martensitic microstructure can be achieved by hot forming and quenching [3]. The Al-Si coating is applied to prevent oxidation during heating and the forming process [3, 4, 10].

2.2 Wear

There are different wear mechanisms, the most common are abrasive wear, adhesive wear, corrosive wear and surface fatigue.

Abrasive wear is the removal of material from a surface. Two-body abrasive wear takes place between two surfaces. The removal of material can result in free surface particles, so two-body abrasion can evolve into three-body abrasion. With three-body abrasion particles are trapped between two surfaces [9]. Since this research is focused on abrasive wear, this wear mechanism is elaborated on in Section 2.3.

Adhesive wear is the adding of material to a surface. Adhesive wear occurs due to strong adhesive bonding between the two bodies. This causes micro-welding, where parts of the sheet metal stick to the tool [9]. Another form of adhesive wear is compaction galling, where wear debris is accumulated in valleys of the tool surface and compacted in the forming process. The wear debris can consist of Al-Si particles from the coating, oxide particles or both. Adhesive wear is a common wear mechanism in sheet metal forming [7].

Corrosive wear is wear resulting from a chemical reaction with one of the two surfaces in contact. Oxidation is a form of corrosive wear, here the chemical reaction is with oxygen [9]. In hot forming processes oxide layers can develop on either the tool or sheet surface.

Surface fatigue, also called delamination, takes place in rolling contacts. Due to repetitive loading, cracks are nucleated below the surface. Further loading and deformation cause the cracks to propagate. When the cracks shear to the surface, long and thin wear sheet delaminate [9].

The wear mechanisms are described separately, however, it is common that they occur alongside each other and they can interact with each other.

2.3 Abrasive wear

2.3.1 Initiation

One would expect abrasive wear to happen at the softest surface. However, in the SMF process abrasive wear can also take place at the tool, which has a harder surface than the sheet. The abrasive wear on the tool can be caused by three body particles or by hard particles embedded in the soft sheet. These particles can be loose Al-Si particles from the coating of the sheet, debris from oxidation, or a combination of both [8].

2.3.2 Stages of wear

Previously, it was assumed that wear increases linearly with the loading duration, which implies a constant wear coefficient. This is in line with the Archard model, which is elaborated on in Section 2.3.3. However, from the research of Behrens et al. [11] three stages of wear can be distinguished:

I Running-in wear

II Steady-state wear

III Accelerated wear

The behaviour of the wear depth and wear coefficient in the three stages is shown in Figure 7. The first stage is running-in, here the wear depth increases rapidly and non-linearly, with a relatively high wear coefficient. The second stage is steady-state wear, where both the wear depth and wear coefficient are fairly constant. The third stage is the accelerated wear, this is where the wear escalates and becomes problematic. The transition between the stages can be induced by external factors or a natural consequence of the materials and tribological system [12].

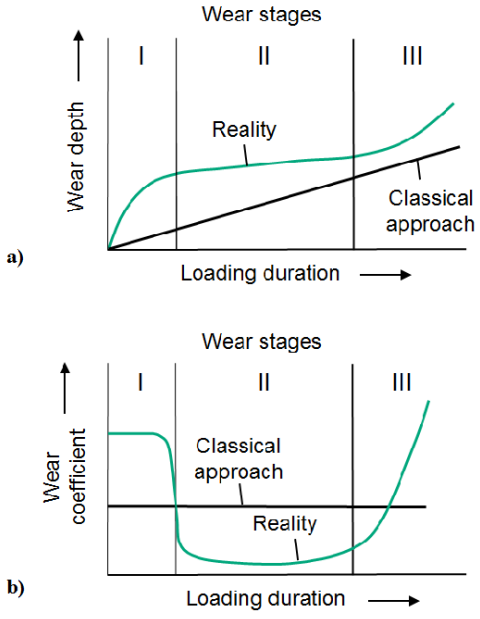

Figure 7: Three stages of wear with a)Wear depth and b)Wear coefficient [11]

Blau [12] concluded that the linear normalisation, the Classical approach in Figure 7, gives a wrong interpretation of the development of wear rates. In their research, a distinction is made between a system specific wear rate (SSWR) and an instantaneous wear rate (IWR). The system specific wear rate is determined over a pre-defined period. This rate is path-independent. The instantaneous wear rate

is determined over a small increment of the operation and can vary a lot during the entire operation. Non-linear wear behaviour has been observed in sliding operations for quite some time, however, is still modelled as a linear process. An incubation stage before the running-in stage can be recognised in some cases, this is illustrated in Figure 8. In the incubation stage the surface can be damaged, but no material is lost. The incubation stage is also called the zero wear stage. The initiation of wear marks the beginning of the wear-in stage. The Archard equation is commonly used for abrasive wear in sliding and assumes a linear relation between sliding distance, normal load, the hardness of the softest material and the wear volume, but does not take the natural transitions into consideration.

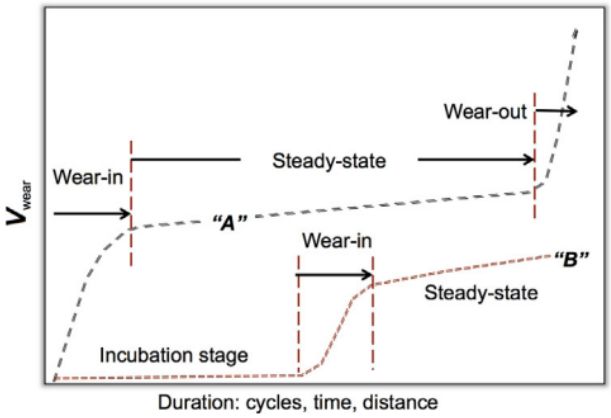

Figure 8: Two curves with non-linear sliding behaviour. Curve A is similar to Figure 7, Curve B has a incubation stage before the wear starts. [12]

In a research of Yuan et al. [13] an interactive friction and wear model is developed to examine tool life prediction for multiple cycles. As mentioned in their research, for sheet metal forming operations often a single cycle simulation is performed, with a constant value for wear and friction. However, in the course of multiple cycles, the rate of wear and friction evolves. The model updates the friction coefficient and the thickness of the coating during thousands of cycles. The model is implemented for a cold forming process and shows the evolution over 500, 1500 and 2000 forming cycles. This shows that using a constant wear rate and friction coefficient is not a correct approach to model multi-cycle loading conditions.

2.3.3 Existing Models

The most common abrasive wear model applied in SMF processes is the Archard model [14]. The Archard model determines the wear based on contact mechanics. The Archard wear equation is shown in Equation 2.

$$V = k \int \frac{F_N}{H} dl \tag{2}$$

Within this equation V is the wear volume, k wear rate, F_N the normal force, H the hardness of the softest surface and dl the sliding length. The amount of tool wear is dependent on the loading conditions and the sliding distance.

The Archard model assumes a linear development of tool wear over the sliding length. However, from Blau [12] and other researches [13, 15] follows that a constant wear coefficient does not suffice to describe tool wear over multiple cycles, since the tool wear develops non-linear.

A variable wear coefficient, or wear rate, is needed to account for the non-linearity. Several non-linear models can be found in literature with a variable wear coefficient. Yuan et al. [13] developed a model that updates the friction coefficient and the coating thickness in the course of multiple cycles, which results in a variable friction coefficient and wear rate. The model was validated with a cold forming case.

The Archard model gives a good indication of the wear locations, but not for the amount of wear. To obtain a quantitative indication of wear, Ersoy-Nürnberg et al. [15] related Archards wear equation to the dissipation of energy. The result is a modified Archard model where the wear coefficient is a function of the accumulated wear work. The wear coefficient is variable, which takes the non-linearity of the wear process into account. The first two phases of wear, running-in and steady-state wear, are recognised in

the experiment carried out with the model. In this model a constant surface hardness is assumed and the model is only tested on cold forming processes.

In literature, no models were found that take the non-linear development of wear into account for hot forming processes.

3 Methods

An experimental data set is provided by Volvo Cars, which includes a tool scan and a simulation file of an A-pillar. The tool scan shows the change of the tool geometry at the end of the lifetime in mm. The tool consists of upper and lower dies. The simulation file gives the possibility to analyse process parameters during forming of the specific part. Similar data sets are provided by other companies and are used within this study to increase the statistical significance of the evaluation. This data is indicated as data set 2.

3.1 Limitations

For the data sets only a scan at the end of the tool life time is available. This means that only a linear approximation of the wear is possible, as illustrated in Figure 9. However, from research it follows that tool wear develops non-linear, see Section 2.3.2. This means the model that is developed cannot capture the tool wear development as it will happen in reality. With just the the state of the tool at the end of its life time, it is not possible to draw conclusions about the interaction between different wear mechanisms, e.g. adhesive wear prior to abrasive wear, in the forming process.

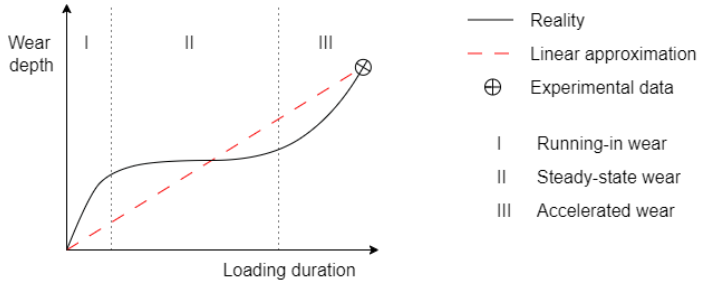

Figure 9: Wear Stages

To compare the simulation data and experimental data, it is important to keep in mind that the simulation shows 1 stroke, while the experimental data shows the amount of tool wear before the tools are refurbished. For the Volvo Cars part this was 170 000 strokes. This means that the value following from the simulation needs to be multiplied with 170 000 - or the experimental value needs to be divided by 170 000 - to make a fair comparison.

Another limitation in the data available is that the locations need to be picked manually in both the tool scan and simulation. It is not possible to export the data from both the programmes and compare them in an automated manner. The manual collecting of the data at the chosen locations is a labour-intensive process and introduces a human error, which is minimised but cannot be eliminated with the current data available.

3.2 Tribological system

This model is set up for a common tribological system in hot forming operations. The material of the tool is the Uddeholm Orvar Supreme, this is an uncoated tool steel 1.2344 (H13), with a surface roughness of $S_a = 0.6\mu m$. The sheet material is the boron alloy 22MnB5 with an Aluminum-Silicium coating, which has a surface roughness of $S_a = 2.0\mu m$. The 3D surface topography of the the sheet and tool material are shown in Figure 10a and 10b, respectively.

The TriboForm library that is used in the AutoForm simulation is a default hot forming library. The sheet is a default boron steel with a Al-Si coating, with $S_a = 2.0\mu m$. The tool is a default tool steel with surface roughness $S_a = 0.6\mu m$. There is no lubrication. The TriboForm library is applicable for a pressure range of 1 - 30MPa, temperatures from 450 - 750°C and velocities from 1 - 300mm/s. The corresponding TriboForm friction model is shown in Figure 10c. 80% of the data points used in this research fall within the pressure range. If the pressure exceeds the range, the TriboForm friction coefficient is determined with a pressure of 30MPa.

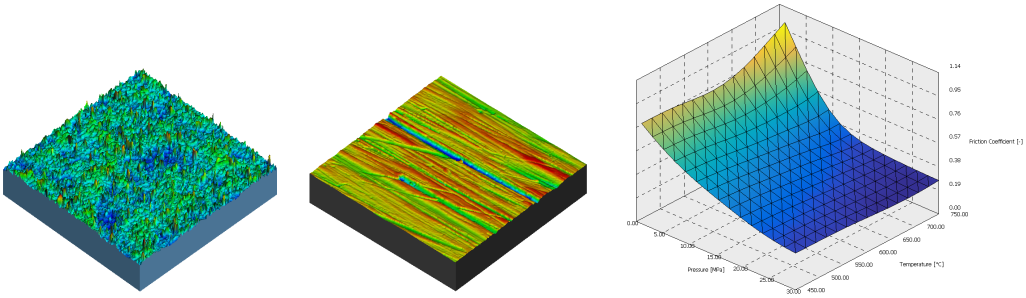

(a) 22MnB5(+AlSi) (b) Tool Steel (c) TriboForm friction model

Figure 10: Surface topographies (a) and (b), and TriboForm friction model (c)

3.3 Workflow

In this section the workflow will be discussed. Several software programmes are used and the workflow is determined by the possibilities and limitations of every programme. First an overview of the programmes is given in Section 3.3.1, to show how they are connected and what their input and output is. Then a research specific workflow is discussed in Section 3.3.2.

3.3.1 Overview

As can be seen in Figure 11, customer data and measured data are the input for the TriboForm software. The customer data consists of the tooling and sheet material characteristics of the tribological system. For the measured data TriboForm executes strip draw tests and confocal measurements. With this data the friction and lubrication conditions can be simulated in the TriboForm software. The Tool Wear model is part of the TriboForm software. The output of the TriboForm software is a customised library, which contains all friction and lubrication conditions for a specific tribological system. This library can be used as an input for the AutoForm software, so tribological characteristics can be incorporated in the forming simulation. Output of the AutoForm software is the projection of the amount of tool wear on the tools.

The experimental data consists of the tool scans, these can be opened with the programme GOM Inspect. In this programme a scan of the virgin tool and the tool before refurbishing are plotted on top of each other. The distance between both scans is calculated and the programme shows the state of tool wear and galling before the tools are refurbished.

With the simulation data out of AutoForm and the experimental data out of GOM Inspect, simulation and reality of the tool wear can be compared. The goal is to adjust the Tool Wear model in such a way that the simulation matches reality.

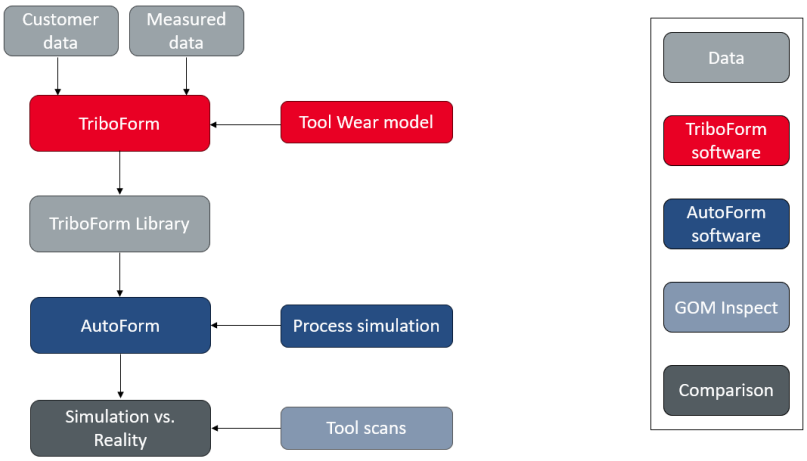

Figure 11: Workflow AutoForm/TriboForm

3.3.2 Detailed workflow

With the workflow in Figure 11, it is only possible to do a visual comparison between the simulation and scan. It is challenging to examine how the existing model can be improved with just the visual comparison, therefore a workflow is set up to obtain numerical values. These values can be analysed in a sensitivity study. Depending on the outcome of this study either the existing model can be improved or a new model can be set up. Once the the best model is found, the model will be calibrated and validated. The research is divided in the following steps:

- Data collection
- Data processing
- Data analysis
- Model setup
- Model calibration
- Model implementation
- Model validation

Every step is explained separately in this section. An overview of the detailed workflow and which software programmes are used in every step is shown in Figure 12.

Data collection

- To compare simulation results with reality, 20 locations on the die are chosen for every data set. These locations have a minimum total sliding length of $0.05mm$. The locations that are selected are a mix of locations with low, medium and high tool wear. This is done so the model accounts for a wide range of tool wear conditions. For the Volvo Cars data, only locations at the upper dies are selected, so the lower dies can be used for the validation of the model.
- Tool wear values are collected from the experimental data in GOM Inspect at the selected 20 locations. To account for the manual picking and resulting location inaccuracy, the average of 10 points in an area of 2x2 mm (+/-1mm) is taken.
- The simulation history of the sliding length, pressure, strain, temperature and velocity is exported out of AutoForm at the chosen 20 locations. To do so, an AutoForm plug-in is created for the mentioned parameters. When running the simulation with the plug-in, the parameter from the sheet is projected onto the tool at every increment in the forming process. The data is collected by exporting the simulation history at the end of the quenching step for all 20 locations.

Data processing

The simulation history of the sliding length, pressure, strain, temperature and velocity are loaded into Matlab. With the imported data other parameters can be calculated. The total sliding length, the incremental contact area, the maximum contact area, the friction coefficient and whether there is contact at all is determined with this data. Also the simulation and experimental data are linked to each other at the corresponding locations.

Data analysis

The data is analysed to find a constant value for the wear rate k in the model that is currently used in TriboForm. Further, a sensitivity study is conducted to see if there is a correlation between process parameters following from the simulation and the amount of tool wear in the experimental data.

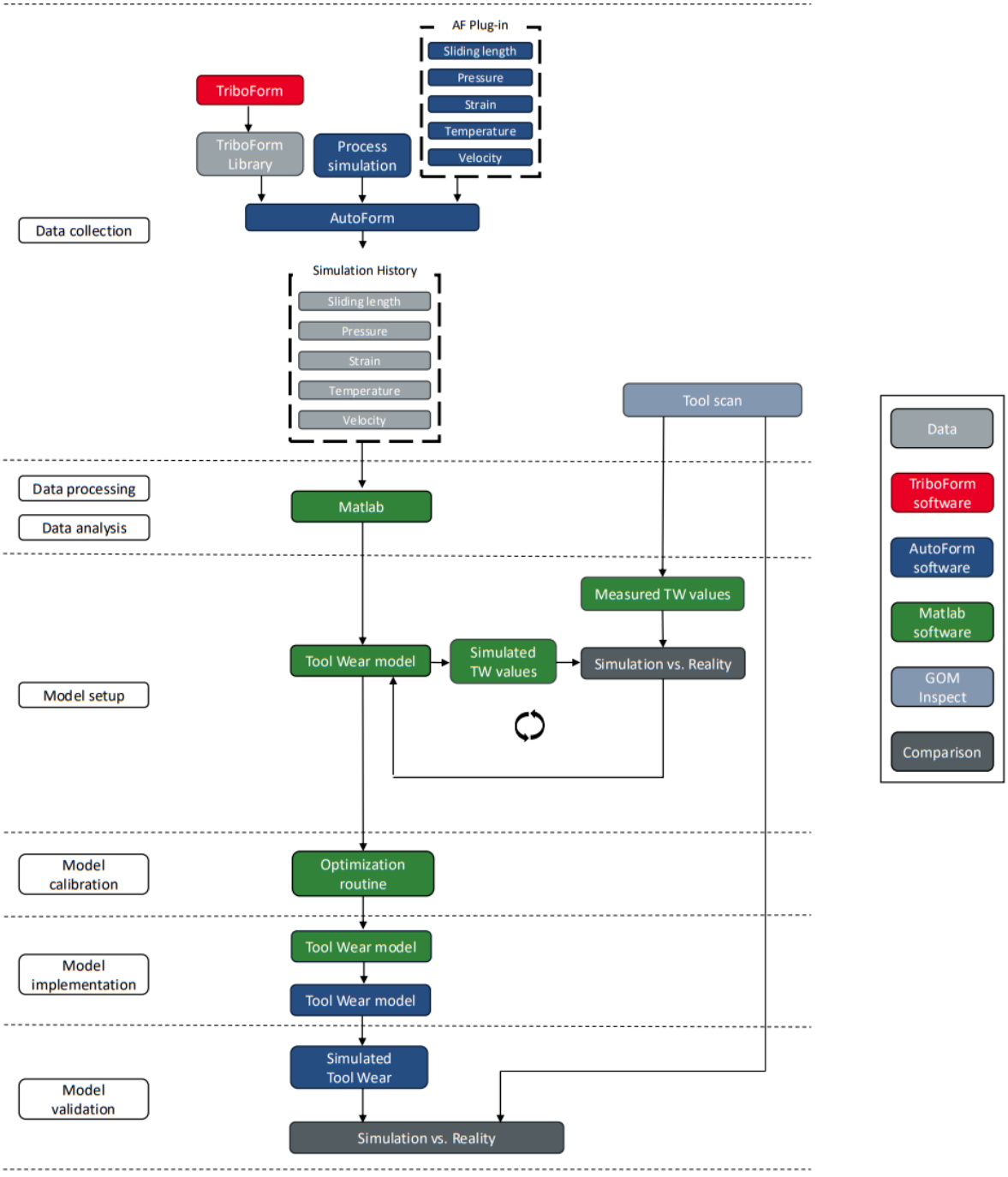

Figure 12: Detailed workflow

Model setup

With the results of the sensitivity study different tool wear models are examined. The basis is the same for all models and shown in Equation 3, where TW stands for Tool Wear, k is the TriboForm(TF) wear coefficient and $model$ is the combination of parameters that could describe the tool wear.

$$TW = k \cdot model \tag{3}$$

Several formulations to determine both the TF wear factor k and the $model$ are examined in Section 4.3. The outcome of the simulated tool wear and the tool wear following from the scan is compared for the different tool wear models. This is an iterative process. Eventually, the most promising model is chosen.

Model calibration

The experimental data is used to calibrate the model. The parameters that need to be determined are found by optimising them for the smallest error with the experimental data.

Model implementation

At this moment the model can be implemented in the AutoForm software with a plug-in. Eventually the model will be incorperated into the TriboForm software.

Model validation

The model can be simulated with a plug-in in AutoForm. To validate the model the tool wear results from the simulation are compared with the tool scan of the lower dies of the Volvo Cars data.

4 Tool Wear model

4.1 Data

4.1.1 Collection

A brief description of how the data collection is executed is given in Section 3.3.2. Figure 13 shows the die of the Volvo Cars A-pillar. In Figure 13a the tool wear on the die is shown. This tool wear follows from two 3D tool scans provided by Volvo Cars. One scan is made before the forming operation started, the other before the tool was refurbished after 170 000 strokes. These scans are plotted on top of each other with a global best fit in the programme GOM Inspect and the surface height deviation shows the tool wear. For convenience these surface height deviation plots are called tool scans from now on. Positive values on the tool scans indicate galling, negative values indicate abrasive tool wear. In Figure 13a the legend and scan are adjusted to only show abrasive wear, since that is the focus of this research. The tool scans with both galling and tool wear are depicted in Figure 27, see Section 7.1. In Figure 13a, the red locations indicate severe tool wear, while the green area's have hardly any wear or galling. From this data set 20 locations are selected. The selected locations are a mix of low, medium and high abrasive wear. At each location 10 points are selected in an area of 2x2mm (+/-1mm) and the average is taken as the tool wear value at that location.

In Figure 13b the corresponding locations are selected in the AutoForm simulation. The locations are checked for the minimum sliding distance of 0.05mm in one stroke. For each of the 20 locations, the simulation history of five different parameters are exported from the tool side. The parameters are the sliding length, contact pressure, temperature, equivalent plastic strain and sliding velocity.

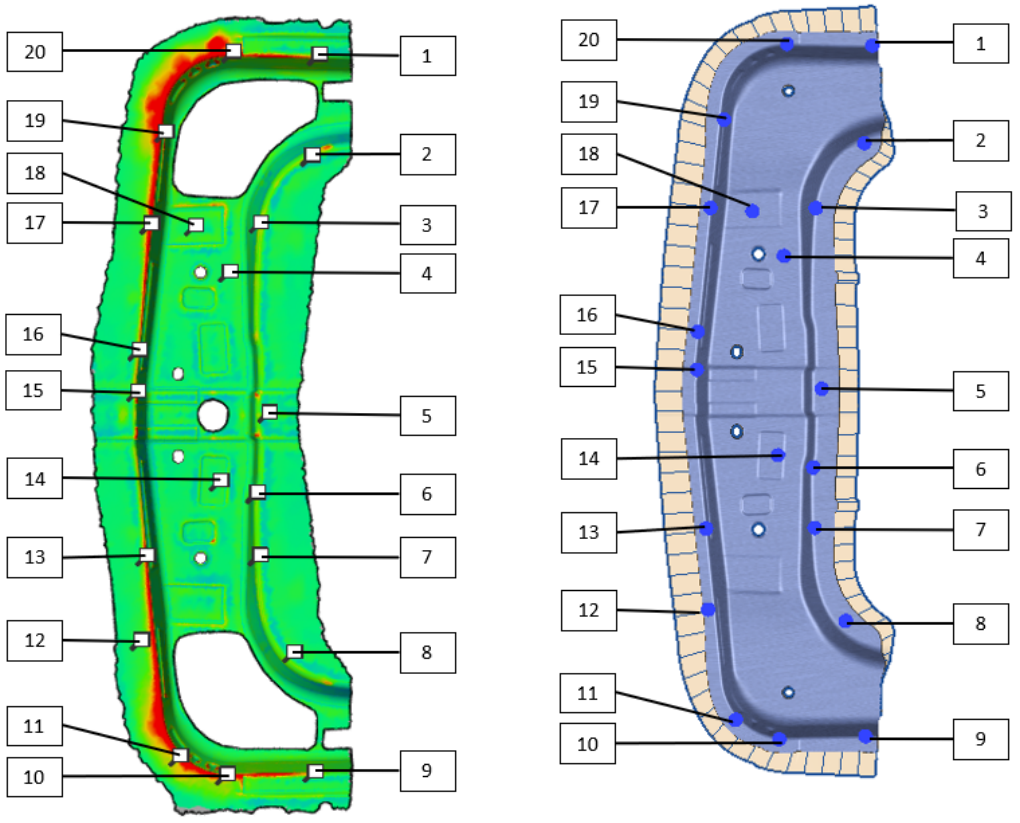

(a) Locations in tool scan

(b) Corresponding locations in the AutoForm simulation

Figure 13: Selected locations on the upper die of the Volvo Cars A-pillar

4.1.2 Processing

The simulation history of the previously mentioned five parameters during one stroke are imported into Matlab for all selected locations. With these process parameters the total sliding length, contact area, friction coefficient and frictional work can be determined. To illustrate the data, the parameters are plotted in Figure 14 for location 1 and 20. The graphs show the change of the parameters during one stroke, which takes approximately 16 seconds and is divided in multiple small time steps. The first 5 parameters are exported from AutoForm and contain the contact pressure, the equivalent plastic strain, the temperature, the sliding velocity and the sliding length of every time step, for the selected locations. The other parameters are determined from the imported data. There is assumed to be contact when the pressure is larger than zero. The 'Contact' plot shows if the tool is in contact with the sheet (1) or not (0). The total length is the accumulated value of the sliding length per time step. The 'ContactAreaInc' is the incremental contact area and determined at every time step. The 'ContactAreaMax' is the maximum contact area the location experienced, this value follows from the incremental contact area, but cannot decrease. For a more elaborate explanation see Appendix C. The friction coefficient is calculated with the pressure, strain, temperature and velocity in accordance with the TriboForm friction model. The frictional work is determined by multiplying the pressure with the friction coefficient and the sliding length at every time step. This value is accumulated over time. The tool wear values from the scan are also imported in Matlab and linked to the process parameters at that location.

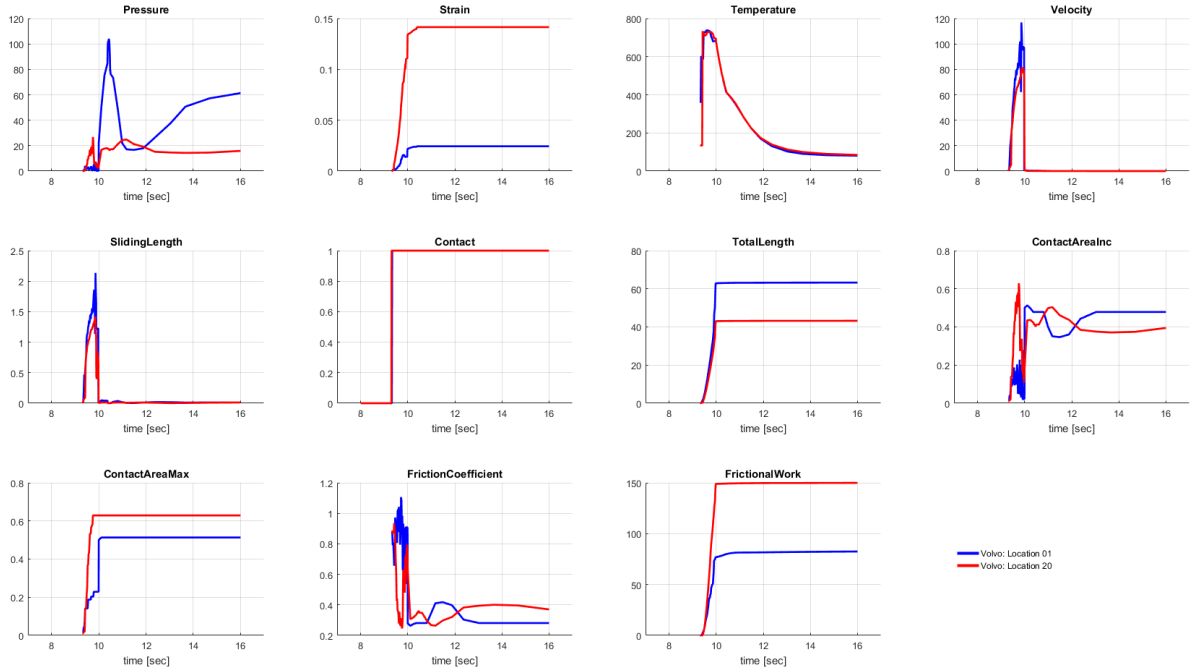

Figure 14: Evolution of multiple parameters during one stroke. Note that the first 5 parameters were exported from the simulation and the latter 6 were determined based on the acquired data.

4.2 Current model

The model currently implemented in TriboForm/AutoForm is based on the Archard model [14], see Equation 4. In this model the real area of contact is multiplied with the wear rate and integrated over the sliding length of one stroke.

$$TW = k \cdot \int \alpha(P, \epsilon, T, \nu) dl \tag{4}$$

For this model an attempt was made to find a constant value for k, the wear rate. This did not give the desired result, see Appendix A. This can be caused by the approximation of the wear rate as a constant or the use of an incorrect model. These causes are further examined in the next sections.

4.3 Model improvement

4.3.1 Sensitivity study

A sensitivity study is conducted to examine possible correlations between the amount of tool wear and process parameters. The parameters that are examined are the total sliding length, accumulated pressure, maximum contact area and the total shear stress. The results are shown in Figure 15, where the blue circles correspond to the 20 locations from the Volvo Cars case. The dashed line is the trend line. Note that TW GOM on the y-axis is the amount of tool wear after 170 000 strokes. From all graphs in Figure 15, a positive correlation between the tool wear and parameter can be recognised. However, the graph with the maximum contact area shows the least scatter, and is therefore most promising.

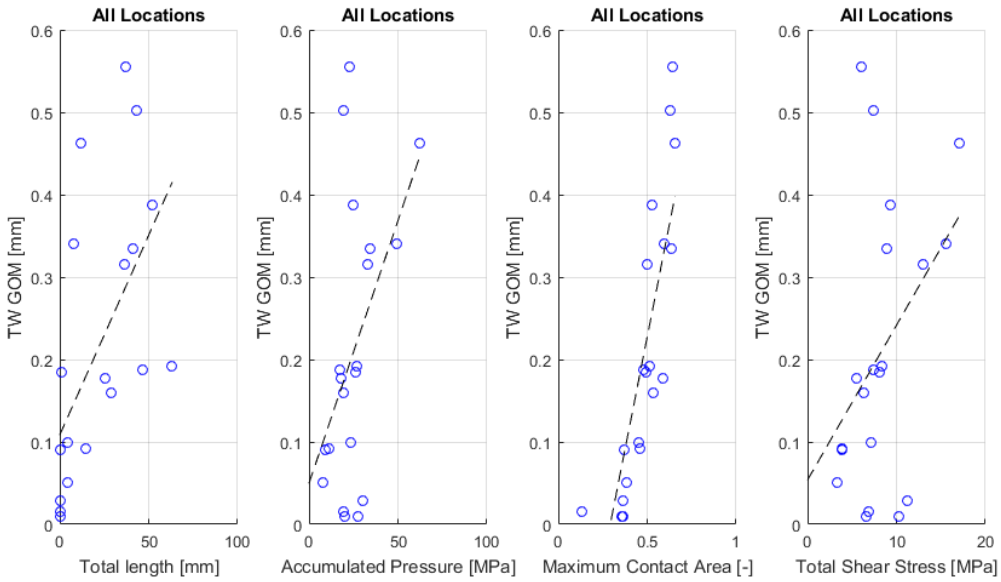

Figure 15: Sensitivity Study

With the results of the sensitivity study in mind, three models are set up. The general formula is given in Equation 5. In this equation, TW is the amount of tool wear, k is the wear rate and $model$ describes the physical model. All models are based on the Archard model [14], since this is the most common model for abrasive wear following from literature [6, 12, 13, 16]. The Archard model determines the amount of wear with a loading condition and the total sliding distance. In the tested models the loading condition differs, but all the models are integrated over the sliding length. The models are discussed below. In Figure 16, the measured and simulated tool wear are plotted against each other for the different models.

$$TW = k \cdot model \tag{5}$$

Pressure

The pressure model, see Equation 6, is a simplified version of the Archard model. In this formulation the hardness of the softest surface is not taken into account. The measured tool wear is plotted against the pressure model in Figure 16a.

$$TW = k \cdot \int Pdl \tag{6}$$

Maximum contact area

The contact area model, shown in Equation 7, is actually the Archard model. In the original Archard model, Equation 2, the normal load is divided by the hardness of the softest surface, which equals the contact area. Flattening is taken into account by using the maximum contact area instead of the

incremental contact area. In Figure 16b, the measured tool wear is plotted against the contact area model.

$$TW = k \cdot \int \alpha_{max} dl \tag{7}$$

Frictional work

The frictional work model, see Equation 8, is based on the dissipation of energy. The model of Ersoy-Nürnberg [15] uses a similar modification of the Archard model, since it is also based on the dissipation of energy. The measured tool wear is plotted against the frictional work model in Figure 16c.

$$TW = k \cdot \int \mu P dl \tag{8}$$

When the model can describe the tool wear adequately, the wear rate k is only needed to scale for the right amount of wear. The wear rate of the models is examined in the next section.

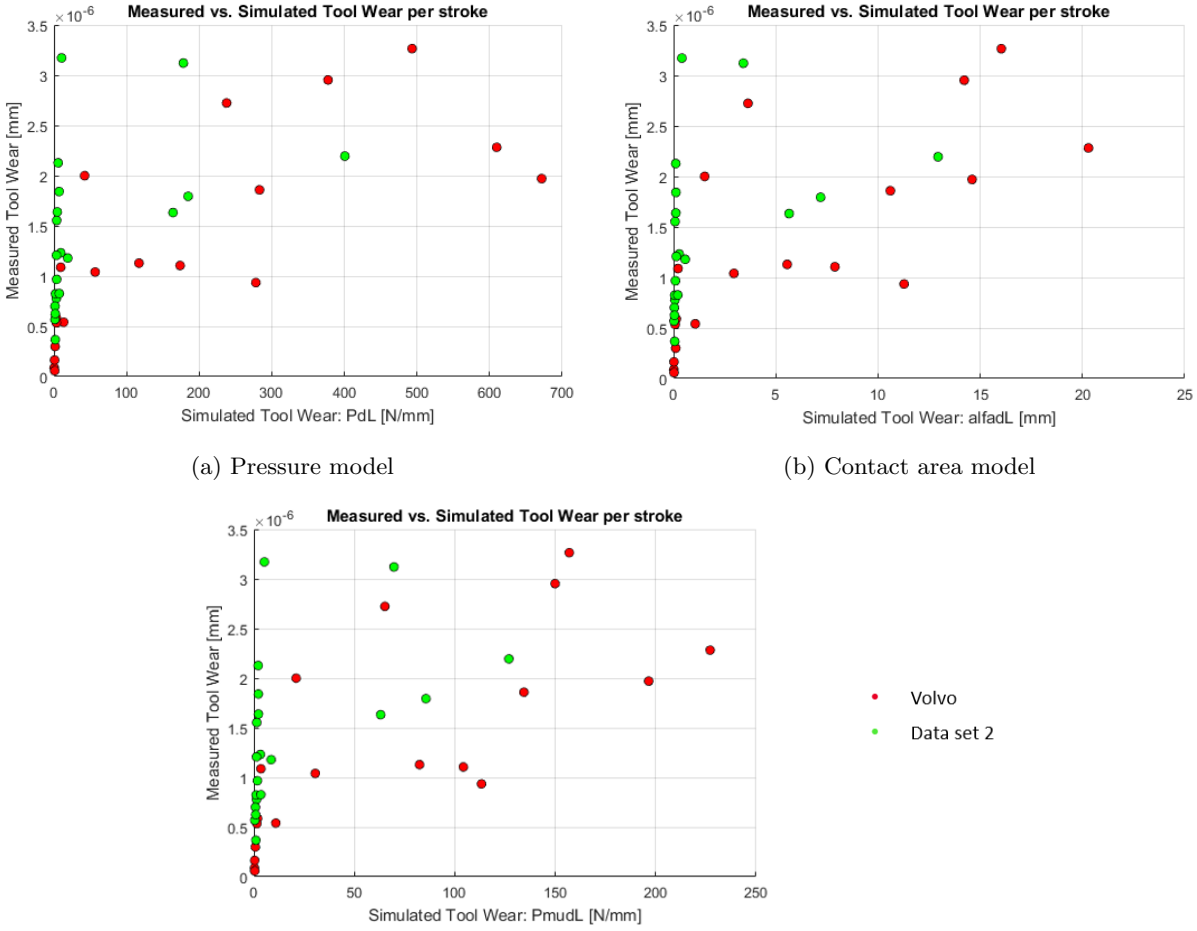

(a) Pressure model

(b) Contact area model

(c) Frictional work model

Figure 16: Measured vs. Simulated Tool Wear per stroke

4.3.2 Wear Rate

The general formula to determine tool wear is given in Equation 5, and can be rewritten to determine the wear rate k, see Equation 9. The wear rate in this equation is called a System Specific Wear Rate (SSWR), following from Blau [12]. The SSWR is determined over a predefined amount of time, in this case over one stroke, and path-independent.

$$k = \frac{TW}{model} \tag{9}$$

The wear rate is determined for the pressure model, the contact area model and the frictional work model for the 20 locations from the Volvo Cars data set. The results are shown in Figure 17.

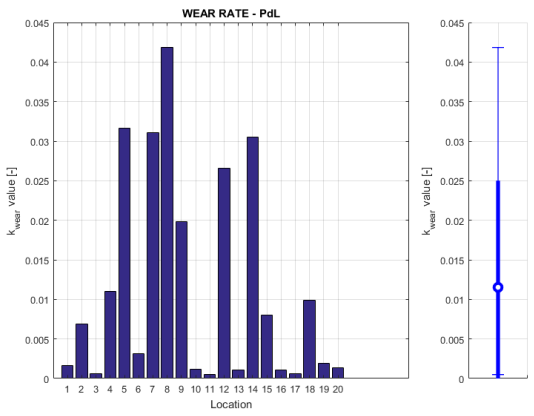

(a) Wear rates pressure model

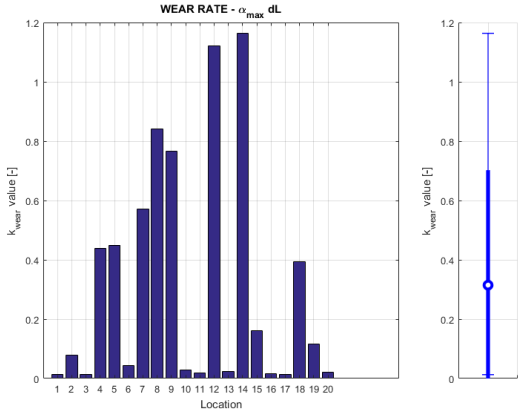

(b) Wear rates contact area model

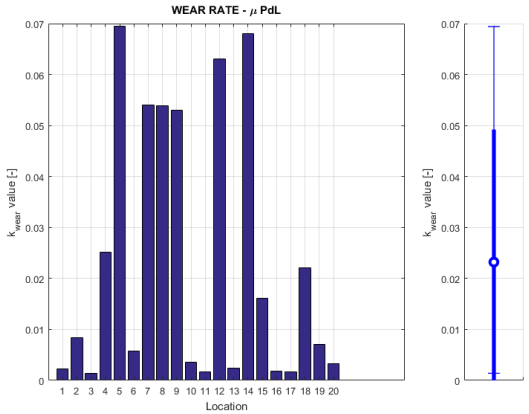

(c) Wear rates frictional work model

Figure 17: Different wear rates k, for different models

From the calculated wear rate values in Figure 17 can be concluded that there is a large variance in wear rate values for all models. Therefore a constant, System Specific Wear Rate may not be suitable to describe tool wear. This can be explained by the nonlinear development of wear. According to Behrens et al. [11], the development of wear consists of three stages and every stage has a different wear rate, see Section 2.3.2. The 20 locations that are selected in the Volvo Cars case can be in different wear stages and therefore all have a different wear rate.

In Figure 16, the measured tool wear from the experimental data is plotted against the simulated tool wear. If the model would describe the tool wear perfectly, all the data points would be located on a straight line. The slope of this line would represent the constant value of k. However, all tool wear models show a nonlinear development of tool wear, which supports the use of a variable wear rate.

To capture the non-linear development of wear, the wear rate k should be adapted. A variable wear rate is introduced, this is called an Instantaneous Wear Rate (IWR) by Blau [12]. This IWR is determined over a small increment of the operation, in this case every time step, and can therefore vary during the process. This variable wear rate will be dependent on the sliding length, because the amount of sliding can be used to make a deviation between different wear stages [12]. This is also supported by Figure 18, because the sliding length follows the same trend as the models in Figure 16. The first two wear stages can be recognised in Figure 18a: running-in and steady-state. The running-in stage shows a rapid

increase in tool wear over a short sliding distance. In Figure 18b a close-up of the 0-2mm range is shown. In the 2-65mm range the tool wear values are much more scattered and the increase in tool wear values is slowed down. This indicates the steady-state stage. See Figure 7 and 9 for reference.

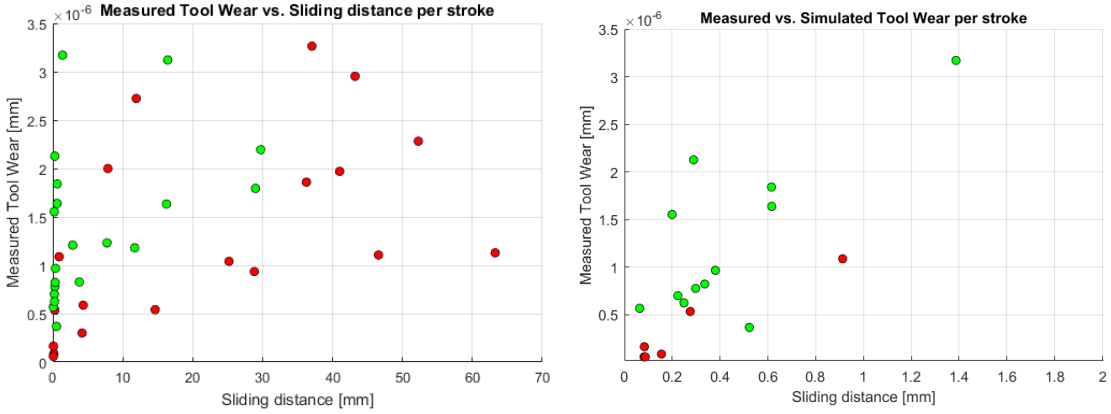

(a) Full range

(b) Close-up: 0-2mm

Figure 18: Measured Tool Wear vs. Sliding distance per stroke

To find a relation between the wear rate k and dl, the wear rate of the experimental data is calculated with Equation 9 and plotted against the total sliding distance of one stroke. For the frictional work model this is shown in Figure 19, the pressure model and contact area model can be found in Appendix B. The red and green dots in Figure 19 represent the locations of the Volvo Cars data set and data set 2, respectively. From Figure 19a it is clear there is a nonlinear correlation between the wear rate k and the sliding distance dl.

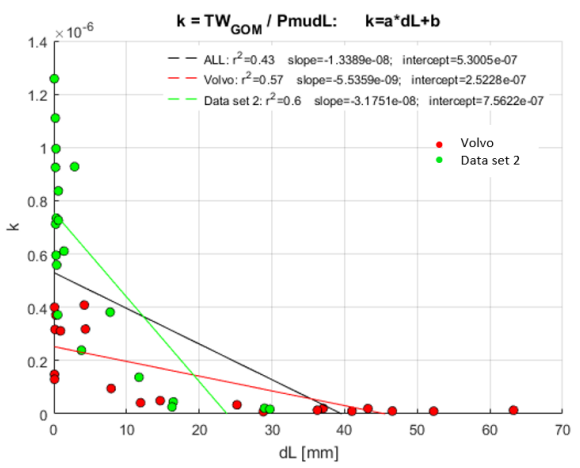

(a) Linear-linear

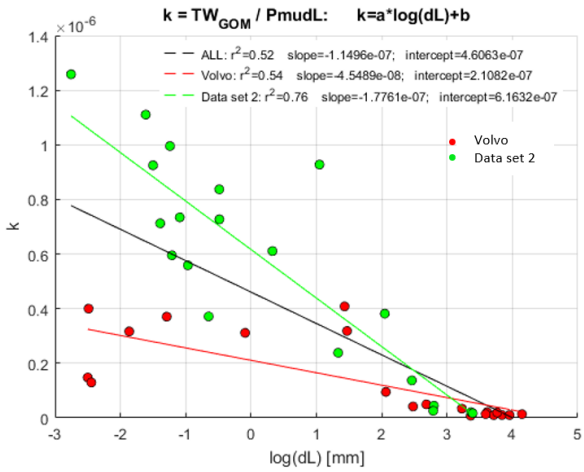

(b) Logarithmic-linear

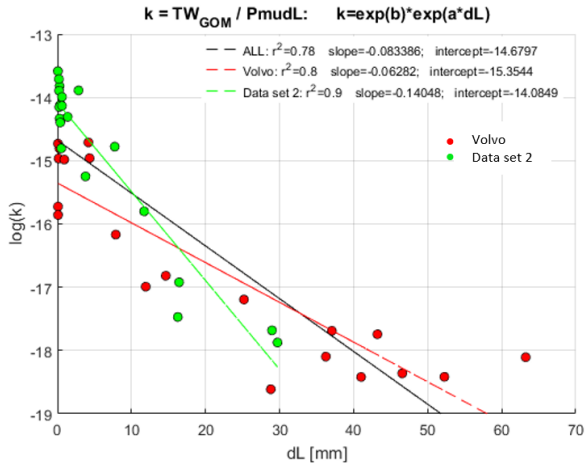

(c) Linear-logarithmic

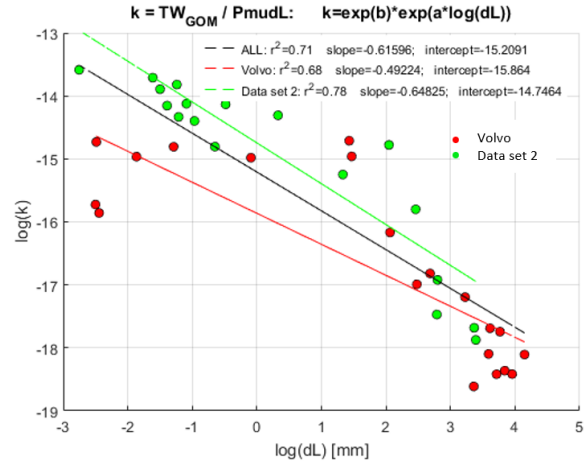

(d) Logarithmic-logarithmic

Figure 19: Wear rate vs. sliding length for the frictional work model, different combinations of linear and logarithmic axis

To examine this nonlinearity, different combinations of linear and logarithmic axis are tested in Figure 19b-d. A linear regression analysis is performed for the Volvo Cars data set, data set 2 and both sets combined. The resulting coefficient of determination(r^2) shows how well the model, in this case the plotted line, fits with the data. r^2 has a value between 0 and 1, where 0 means that the model does not fit with the data at all and 1 means that the data fits perfectly with the model. The aim is to find the linear or logarithmic relation with the highest coefficient of determination. The results are shown in Table 1 to 3, the highest value is bold.

Coefficient of determination - $\int Pdl$				
Data set	linear-linear	log-linear	linear-log	log-log
All	0.48	0.57	**0.76**	0.70
Volvo Cars	0.53	0.50	**0.74**	0.64
Data set 2	0.68	0.81	**0.92**	0.78

Table 1: Pressure model

Coefficient of determination - $\int \alpha_{max} dl$				
Data set	linear-linear	log-linear	linear-log	log-log
All	0.40	0.58	**0.78**	0.77
Volvo Cars	0.56	0.71	**0.80**	0.78
Data set 2	0.58	0.85	**0.92**	0.83

Table 2: Contact area model

Coefficient of determination - $\int \mu Pdl$				
Data set	linear-linear	log-linear	linear-log	log-log
All	0.43	0.52	**0.78**	0.71
Volvo Cars	0.57	0.54	**0.80**	0.68
Data set 2	0.60	0.76	**0.90**	0.78

Table 3: Frictional work model

For all data sets and all models the definition of k with the sliding length on a linear x-axis and the value of k on a logarithmic y-axis gave the highest coefficient of determination. This resulted in the TriboForm wear coefficient, which is shown in Equation 10b.

$$log(k) = a \cdot dl + b \tag{10a}$$

$$k = e^{b} \cdot e^{a \cdot dl} \tag{10b}$$

4.3.3 Different models

The different models are plotted with the TriboForm wear coefficient and compared. The model with the highest coefficient of determination is the final model, the results are shown in Table 4.

Data set	Coefficient of determination		
	Pressure	Contact area	Frictional work
All	0.76	0.78	0.78
Volvo Cars	0.74	0.80	0.80
Data set 2	0.92	0.92	0.90

Table 4: Comparison of different models

From Table 4 follows that contact area and frictional work model give a similar coefficient of determination and both perform slightly better than the pressure model.

However, the contact area model cannot be used for this application. In AutoForm the sheet history of the contact area is available and with postprocessing the correct contact area can be determined. However, within the data that is exported out of AutoForm for this research, the sheet history is not available. Therefore no physically correct approximation of the contact area can be made and the use of the contact area in the model cannot be substantiated. In Appendix C the subject is explained in more detail. If the correct contact area could be determined it would be an interesting model to examine further.

Next to this model, the frictional work model describes the experimental data best, since it has the highest coefficient of determination, see Table 4.

4.4 Final model

The frictional work model is most suitable to describe abrasive tool wear. The final model is formulated in Equation 11. Tool Wear (TW) is replaced by wear depth (h_{wear}) in this formulation, as this is the most practical way to visualise and examine tool wear.

$$h_{wear} = \int k(dl)\mu(P, \epsilon, V, T)Pdl \tag{11}$$

$$k = e^{b} \cdot e^{a \cdot dl} \tag{12}$$

With the TriboForm wear coefficient in Equation 12 substituted into Equation 11, the final model is given in Equation 13.

$$h_{wear} = e^{b} \int e^{a \cdot dl}\mu(P, \epsilon, V, T)Pdl \tag{13}$$

In the next chapter a calibration procedure is performed for this model, to determine the best values for a and b.

5 Calibration

The formulation of the frictional work model is shown in Equation 14. The values a and b of the TriboForm wear coefficient in Equation 14b still need to be calibrated. This is done by fitting the parameters for the smallest error with the experimental data. The model can be used for different tribological systems. For every type of system a calibration of a and b should be carried out, the calibration is tribology system specific.

$$h_{wear} = \int k(dl)\mu(P, \epsilon, V, T)Pdl \tag{14a}$$

$$k = e^{b} \cdot e^{a \cdot dl} \tag{14b}$$

This tribological system has an 22MnB5 sheet with an AlSi coating, the tool is an uncoated tool steel 1.2344 and the system does not have a lubricant. All experimental data available for this system is used for the calibration, so both the data of the Volvo Cars upper dies and data set 2, to increase the statistical significance.

The values for a and b are found with the fmincon function in Matlab, which applies the interior point method. A start point, upper and lower bound are set. The function minimises for the smallest error, in this case the Root Mean Squared (RMS). The RMS takes the square root of the average squared error. This error is determined by the difference between the simulated and measured values. When the RMS equals zero the simulation and measured values are a perfect fit. The aim is to find a value for the RMS that is as close to zero as possible. The optimisation process is plotted in Figure 20.

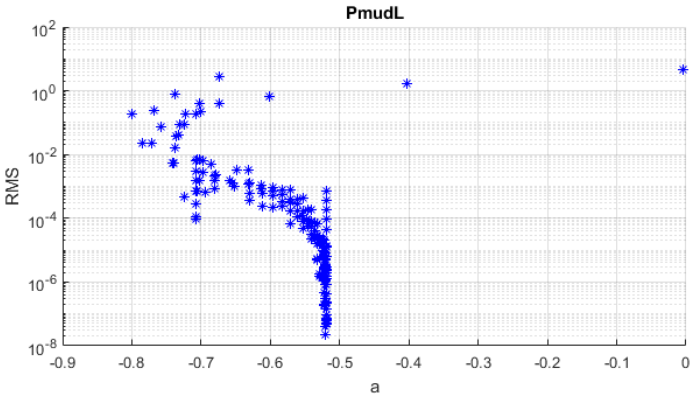

(a) Calibration of a

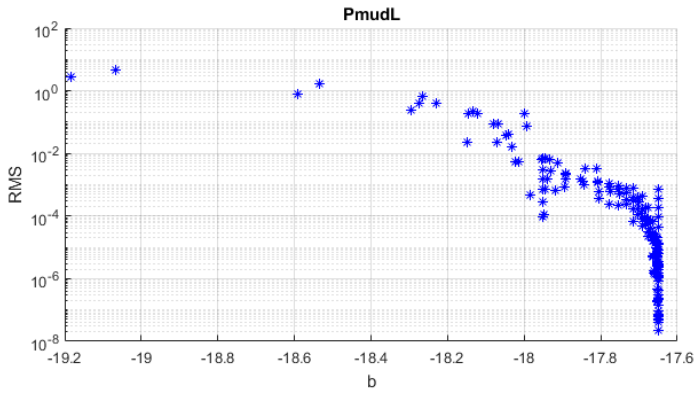

(b) Calibration of b

Figure 20: Calibration of a and b

The optimisation resulted in the following values for a and b, see Equation 15.

$$a = -0.519043 \tag{15a}$$

$$b = -17.6496 \tag{15b}$$

This results in the following formulation for the final model, see Equation 16. The relation of k with the sliding length is shown in Figure 21. As can be seen in this figure, the wear coefficient decreases significantly with an increasing sliding length.

$$h_{wear} = \int k(dl)\mu(P, \epsilon, V, T)Pdl \tag{16a}$$

$$k = e^{-17.65} \cdot e^{-0.52 \cdot dl} \tag{16b}$$

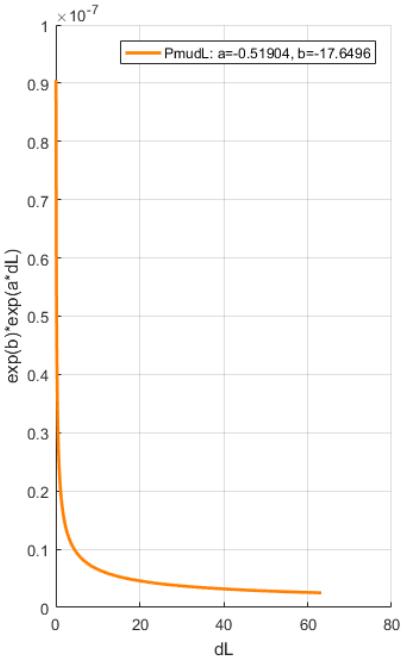

Figure 21: k vs. sliding length

With Equation 14b substituted in 14a the final model for this tribological system is given in Equation 17.

$$h_{wear} = e^{-17.65} \int e^{-0.52 \cdot dl} \mu(P, \epsilon, V, T)Pdl \tag{17}$$

6 Validation

6.1 Tool Wear

In the previous sections, a tool wear model has been developed. This model is based on the data acquired from the upper dies from the A-pillar of Volvo Cars. In order to validate the developed tool wear model, a different tool has been selected. The validation is carried out with the lower dies and blankholder from the A-pillar of Volvo Cars. An overview of the tools is given in Figure 22a. The isometric view of the validation part is shown in Figure 22b. The validation part consist of two parts and this is visible in the scan, the black line separates the lower dies and blankholder.

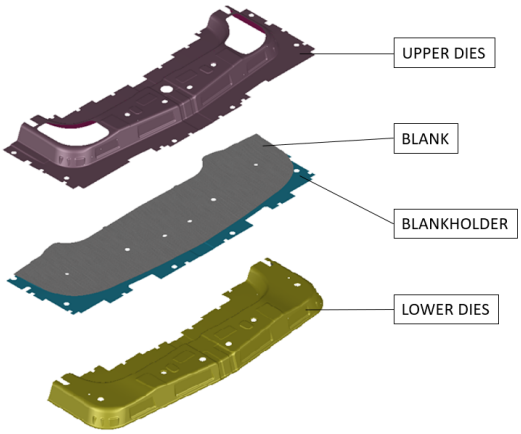

(a) Tools

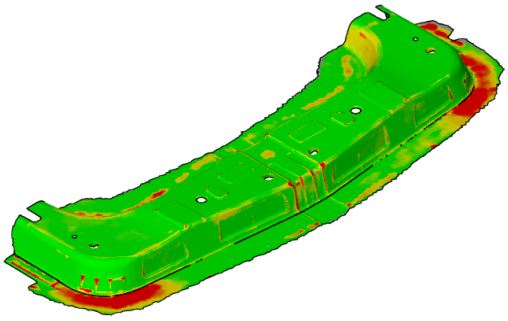

(b) Tool scan of the validation part: lower dies and blankholder

Figure 22: Volvo Cars A-pillar

The tool scan shows the tool wear after 170 000 strokes, but the model simulates the tool wear after 1 stroke. To make a fair comparison, a plugin is created where the tool wear in the simulation is multiplied with 170 000 to match the scan. The result is shown in Figure 23. A closer look will be taken at the areas in the black and blue frame, in Figure 24 and 25, respectively.

In Figure 24, a close up of the black frame in Figure 23 is presented. Figure 24a shows the measured tool wear values from the experimental data, Figure 24b shows the simulated tool wear values following from the TriboForm wear model. The tool wear is analysed for five different areas, these areas are indicated in Figure 24b.

The measured and simulated tool wear in area 1 and 2 of Figure 24a show a good agreement. The simulated tool wear in area 3 and 4 is underestimated by a factor 10. It is important to note that these areas are located in the convex part of the die, and therefore experience a minimum amount of sliding. The tool wear values in area 5 are in the same order of magnitude as the values from the tool scan, but slightly off.

A striking part is the striped pattern in area 2 of Figure 24b. This pattern is caused by the wrinkles of the sheet, which leads some parts of the sheet to be in contact with the tool while others are not. During thousands of strokes the parts in contact will alternate. However, because the simulation only covers 1 stroke and is subsequently multiplied with the total amount of strokes, the displacement of the areas in contact is not captured. In the actual manufacturing process, every part of the area will be in contact at some point. Therefore the entire area will experience wear, as can be seen in the tool wear scan.

In Figure 25 a closer look is taken at the blue frame from Figure 23. Similar trends are observed here. The tool wear values in area 6, 7 and 8 are underestimated in the simulation by a factor 10. These areas are also located on the convex part of the die and experience significantly less sliding than the other locations. The tool wear values predicted in area 9 are a bit off, but in the right order of magnitude.

With respect to the locations where abrasive tool wear occurs, the TriboForm wear model is able to provide an accurate prediction. The model is also able to give a solid quantification of the tool wear, with the exception of areas with a minimal amount of sliding distance. Possible causes for this underestimation are discussed in Section 7.3.

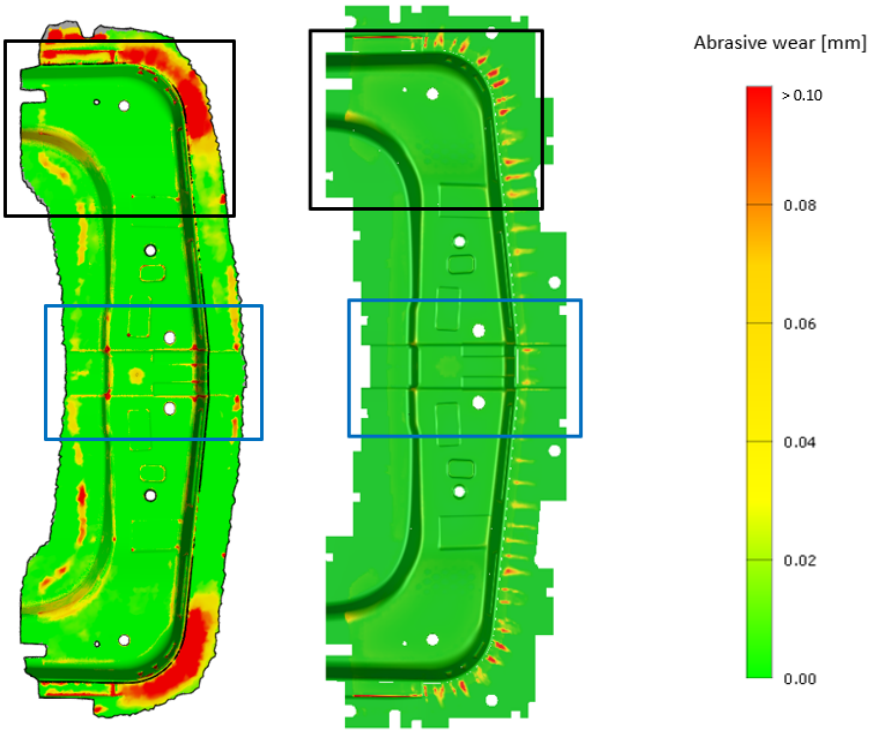

(a) Measured tool wear (b) Simulated tool wear

Figure 23: Comparison tool wear in scan and simulation after 170000 strokes

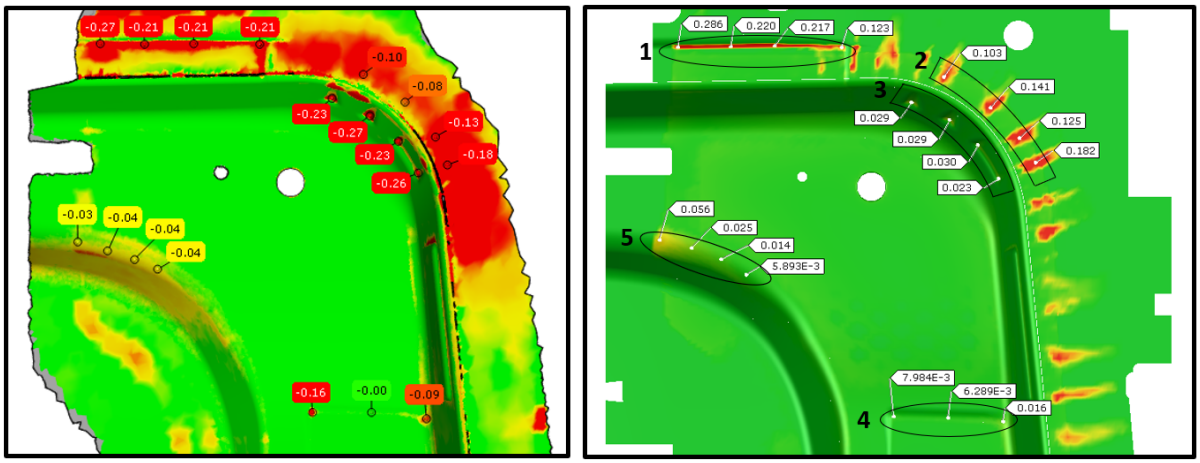

(a) Measured tool wear (b) Simulated tool wear

Figure 24: Comparison tool wear in scan and simulation - black frame

6.2 Tool life time

The tool life time, or production volume, is of interest for the manufacturer in order to schedule refurbishing or replacement of the tool. With the amount of tool wear in one cycle and a critical value for the tool wear, the abrasive wear limit, the amount of cycles before the tool needs to be refurbished can be determined. For the Volvo Cars case the abrasive wear limit is set to $0.25mm$, this resulted in the production volume plot in Figure 26. According to the simulation, the main part of the die would be suitable to produce up to a million parts. However, the parts with a lower production volume determine the tool life time. Some production volume values are displayed in Figure 26b. The areas with the lowest values indicate that about a 150 000 parts can be produced before refurbishing is needed. The tools in

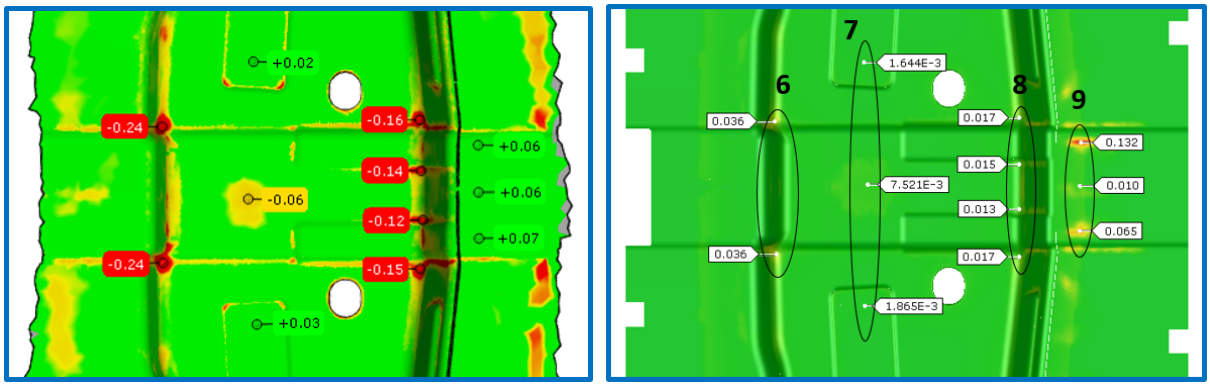

(a) Measured tool wear (b) Simulated tool wear

Figure 25: Comparison tool wear in scan and simulation - blue frame

the Volvo Cars case are refurbished after 170 000 strokes. Therefore the simulation gives a fairly close estimation.

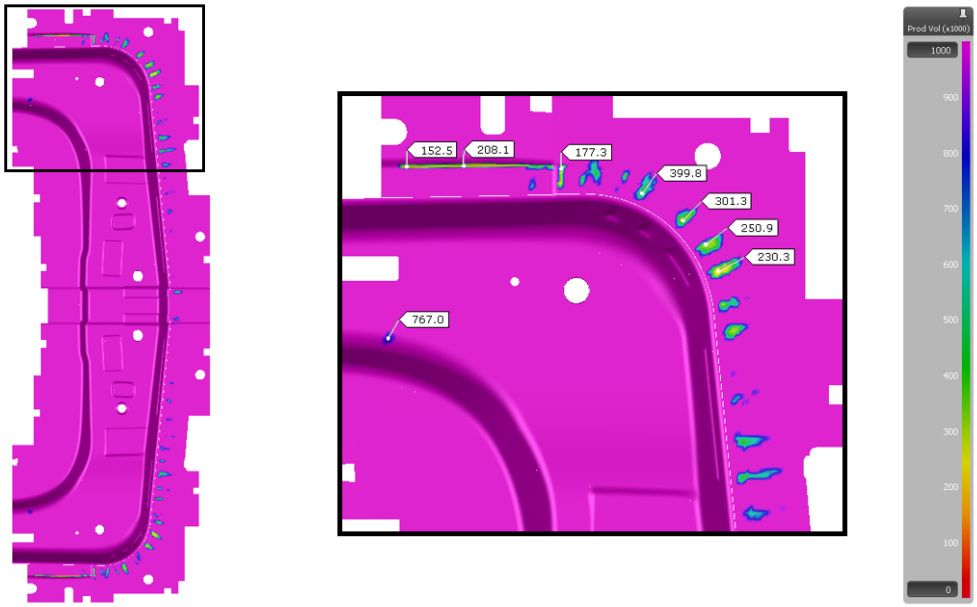

(a) Overview (b) Black frame

Figure 26: Production volume (x1000) based on maximum tool wear depth

7 Discussion

In this chapter, possible explanations for deviating results are discussed. Also some considerations about the research in general are elaborated on.

7.1 Combined wear mechanisms

First of all, one should be aware that this research focuses on abrasive tool wear exclusively. Other wear mechanisms are outside the scope of this research. However, from research it follows that different wear mechanisms can occur alongside each other and interact with each other. The main wear mechanisms in hot stamping are abrasive wear and galling. For the Volvo Cars case this is visible in Figure 27. Galling occurred in the blue areas, where sheet material is added to the tool surface. An interaction that is observed by Venema et al. [7] is abrasive wear followed up by compaction galling at temperatures above 600 °C. Since there is only a scan of the tool available just before refurbishing, it not possible to say if interactions between the wear mechanisms took place. In this research only the abrasive wear is taken into account, but for an accurate representation of the wear during the forming process the interaction of the wear mechanisms should be considered as well.

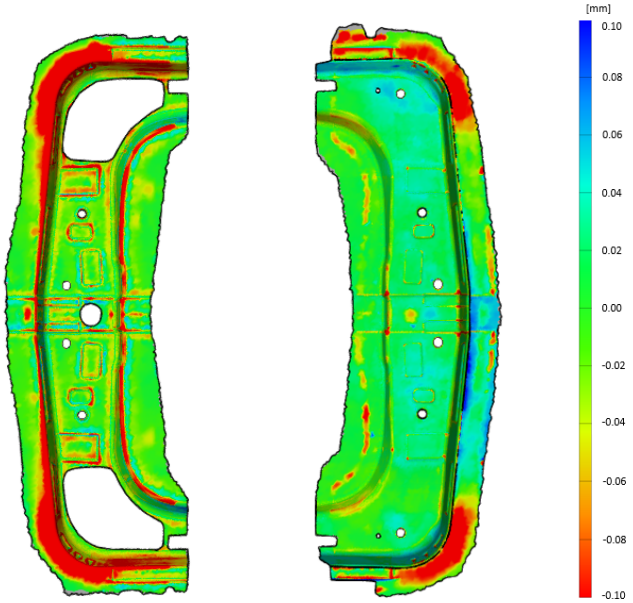

(a) Upper die (b) Lower die

Figure 27: Tool scan of Volvo Cars A-pillar, with galling(blue areas) and tool wear(red areas)

7.2 Linear approximation tool wear

As discussed in Section 2.3.2 the development of tool wear is non-linear and consists of three stages. Figure 9 showed that the experimental data is only available at the end of the third stage, and therefore only a linear approximation of the tool wear seemed possible. This is carried out by simulating the tool wear after one stroke in AutoForm, and multiplying this amount by the number of strokes. However, to obtain a good estimation in the simulation, the non-linearity is included in the model via the wear coefficient k. The wear coefficient is made dependent on the sliding distance in one stroke and therefore variable. By including the sliding distance it is possible to distinguish the different stages and match the wear coefficient accordingly. The final model has a linear relation over multiple strokes, but a non-linear approximation within one stroke.

7.3 Deviating tool wear values

From the validation case in Section 6.1 followed that the amount of tool wear is underestimated in specific parts of the tool. A distinction can be made between the parts where the model estimates the correct amount of tool wear and the parts where the model underestimates the amount of tool wear by a factor 10. The parts with the correct estimation are located on the edges, the lower flat regions, of the tool. The underestimated parts are located in the 'convex' parts, so the higher regions, of the tool. In Figure 28 several locations are selected and the corresponding simulation history is plotted in Figure 29 to examine the differences between the higher and lower regions of the tool. In Figure 28, locations 1, 2 and 3 are in the lower region and result in a correct estimation of the tool wear. Locations 4, 14 and 18 are in the higher region and are a factor 10 off from the actual tool wear amount. The simulation history of the parameters for the selected locations are plotted in Figure 29.

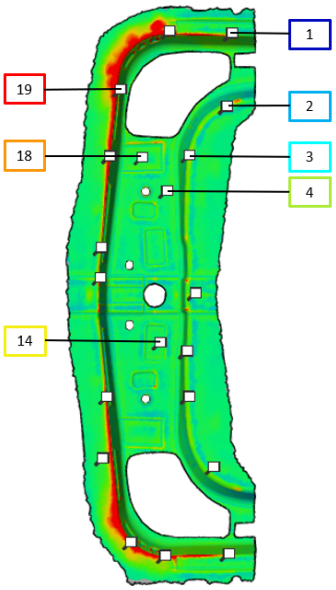

Figure 28: Selected locations Volvo Cars die

From Figure 29 several observations can be made. The first is that the underestimated locations 4, 14 and 18 are in contact later than the others. This also results in a significantly lower sliding distance. The locations 4, 14 and 18 all have a total sliding distance of approximately $0.08mm$, while the others vary from $15mm$ to $63mm$. The values of the friction coefficient are not deviant for locations 4, 14 and 18, but the pressure does not exceed 16MPa while the other locations experience higher pressures. The lower values for the sliding distance and pressure result in a low value for the frictional work and therefore a low estimation of the tool wear amount. The nonlinear formulation of k should account for the lower value following from the low sliding distance, but this seems insufficient. This can be caused by the data selected for the calibration. Only 4 of the 40 data points have a sliding distance smaller than $0.1mm$. To improve the tool wear prediction of the parts with a low sliding distance, the amount of data points with this characteristic should be increased in the calibration set. This way the TriboForm wear coefficient can presumably account for the underestimation of these tool wear values.

Another explanation for the underestimation is that the tool experienced deformation due to the high pressure and this was interpreted as tool wear. To examine this, location 19 is added to Figure 28. This location is similar to the locations in area 2 of Figure 24b in Section 6.1. In Figure 29 can be seen that location 19 experiences high pressures, up to 110MPa. Also high strain is observed for this location, but it is important to note this is the strain of the sheet projected on the tool. The tool is assumed to be rigid and can therefore not deform in the simulation.

Figure 30b shows a close up of area 3 from Figure 24 with an adjusted legend. The area is indicated with the dashed frame in Figure 30a. The legend in Figure 30b shows both positive and negative values. The negative values indicate a decrease in surface height over the 170 000 strokes, the positive values imply an increase in surface height. It is eye-catching that the surface height decreased on the ribs, but

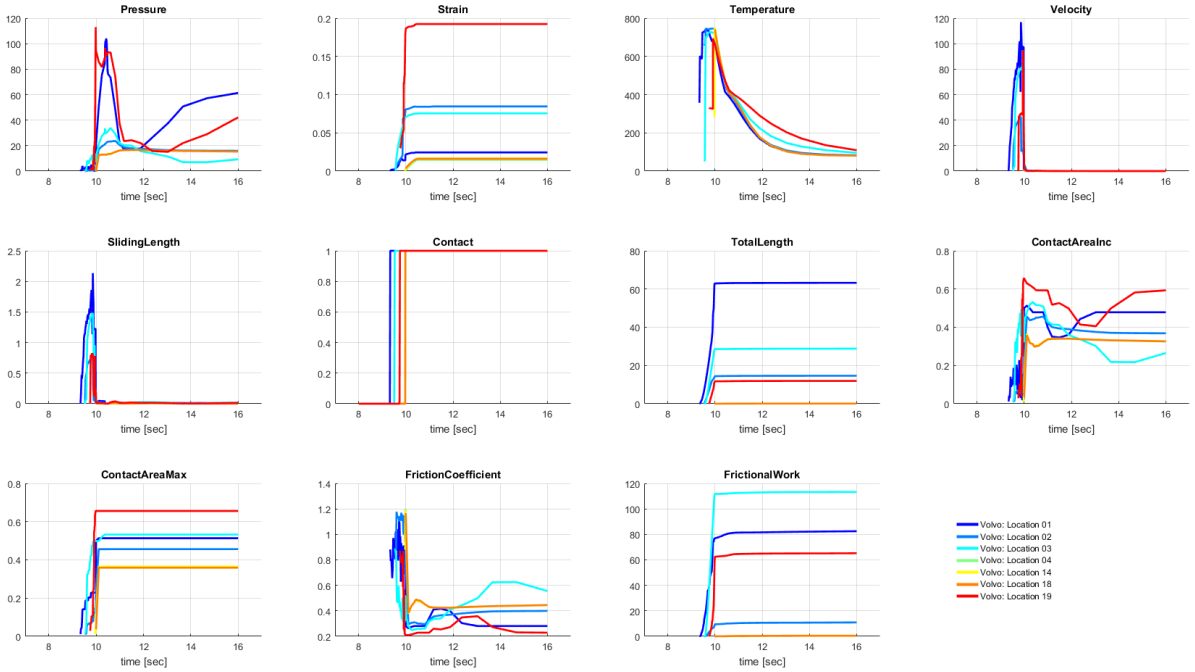

Figure 29: Simulation history of parameters for selected locations

increased in the area around these ribs. In terms of tool wear this would suggest that the abrasive wear on the rib is surrounded by galling around the rib. Another explanation for this surface deformation could be that the high contact pressure on the rib resulted in a redistribution of the ribs material around the rib. This would imply that the rib is plastically deformed and the tool cannot be considered to be fully rigid. In that case a different phenomenon took place, and it is a logical consequence that this is not captured by the tool wear model.

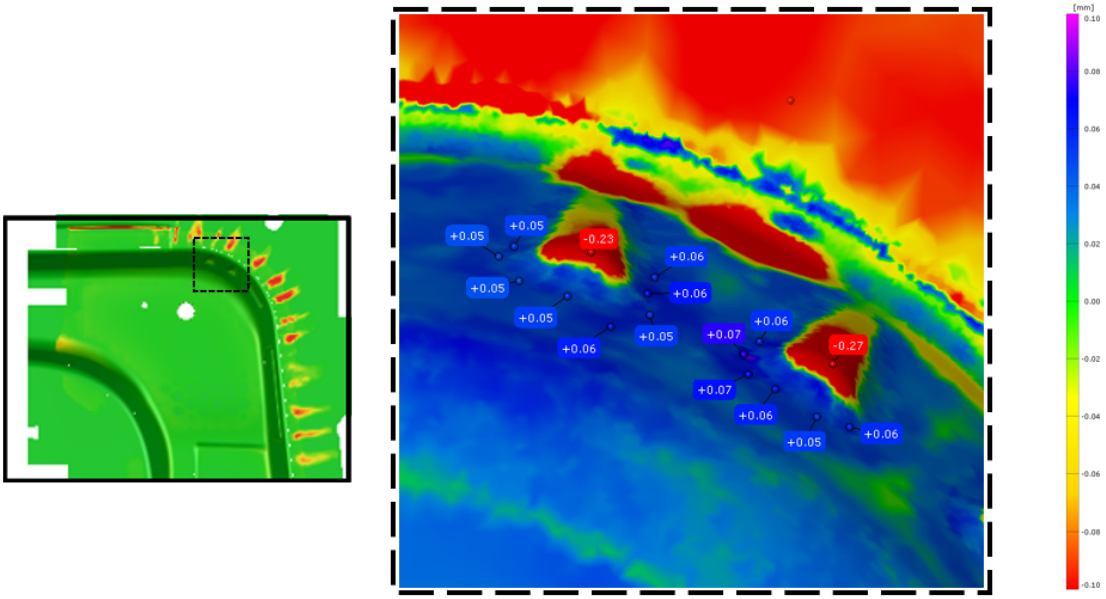

(a) Figure 24 with dashed frame

(b) Close up of the dashed frame

Figure 30: Close up of area 3 from Figure 24, with an adjusted legend

8 Conclusion

In this research, a model that can successfully predict the locations and severity of abrasive wear in hot forming is developed. A literature study into existing wear models is conducted. With the experimental data provided by Volvo Cars, a sensitivity study is carried out to examine the relation between process parameters and the amount of abrasive tool wear. This resulted in several potential models. The models were tested and the frictional work model, based on the dissipation of energy, showed the highest potential. This model is calibrated on the available experimental data and validated with a case. The validation showed that the model is able to the predict the locations that will experience abrasive tool wear very well. For locations with a significant sliding distance the amount of tool wear is predicted accurately. At locations with a low sliding distance the tool wear is under-predicted. To solve this underestimation of the amount of tool wear, an adjustment to the calibration procedure is proposed. The model can be used to predict the tool production volume and can identify critical areas in the tool, which can be used to increase the tool life time.

9 Recommendations

This research resulted in a promising abrasive tool wear model and some interesting observations. In this chapter, recommendations for improvement of the developed model and possible future research topics are discussed.

9.1 Nonlinear development tool wear

Tool wear develops nonlinearly with the number of strokes [11, 12]. For this research, a scan was made of the virgin tool and just before the tool was refurbished, so at 'the end' of the tool life time. The tool wear values that follow from this data show the amount of tool wear in the tool life time, but not the development of the tool wear. Therefore, a linear development of tool wear over the tool life time is assumed in this research. The nonlinearity of the tool wear is included within one stroke by applying the TriboForm wear coefficient in the model. It would be interesting to map the nonlinear development over thousands of strokes by making tool scans at several points in between the start of manufacturing and before refurbishing is needed. This way the nonlinear development that is simulated in the model can be checked, and possibly improved, with experimental data.

9.2 Combine galling and tool wear models

Both galling and tool wear occur during hot forming processes. At this moment there are two separate models available to simulate these wear mechanisms. To improve the user experience, it would be valuable to combine these models and show galling and tool wear in one simulation. This can be done by plotting the results in the same simulation. However, this would only account for the situation where the wear mechanisms occur alongside each other, and disregard the interaction between them. The research that is proposed in Section 9.1 could help to give an insight in the interaction between the wear mechanisms and can help to develop a combined model.

9.3 Tool deformation in simulation

In the current forming simulations in AutoForm, the tools are modelled as rigid. This means that deformation of the tools is not taken into account in the forming process. It would be interesting to follow the deformation of the tool over thousands of cycles. The nonlinear development of tool wear, the different wear mechanisms and deformation due to contact forces could be included. A similar simulation is available for the temperature distribution of the tools in cold forming. A disadvantage of this way of modelling is that the computational time increases significantly, but it would give valuable insight in the development of tool wear in the course of thousands of cycles and the influence on the product.

9.4 Contact Area

As described in Section 4.3.3 and Appendix C, the contact area cannot be used, because it is not determined correctly for this application. If the sheet history can be obtained to determine the accurate maximum contact area, either in the model or in the post processing step, it is of interest to examine this model. The Archard model is widely used and it would be valuable to make a fair comparison to the model that is developed in this research.

9.5 Improve data export options for tools in AutoForm

For the development of the tool wear model it was a challenge to obtain the tool wear data from the AutoForm software. The needed parameters were simulated with a special plugin and manually exported for every location. The manual picking of the locations and exporting the relevant parameters was a labour-intensive process and prone to errors. When the tool data would be available in a STL file, the model could be based on a larger data set. This would improve the quality of the model and accuracy of the calibration significantly. This export option is already available for the sheet data and would be useful for the calibration of future tool wear models.

References

[1] E. Kooistra. Prediction and validation of galling behavior in hot sheet metal forming processes, March 2021.

[2] J. Hol, M.V. Cid Alfaro, M.B. de Rooij, and T. Meinders. Advanced friction modeling for sheet metal forming. *Wear*, 286-287:66 – 78, 2012. Cited by: 82; All Open Access, Green Open Access.

[3] H. Karbasian and A.E. Tekkaya. A review on hot stamping. *Journal of Materials Processing Technology*, 210(15):2103 – 2118, 2010. Cited by: 1431.

[4] J. Hardell and B. Prakash. High-temperature friction and wear behaviour of different tool steels during sliding against al-si-coated high-strength steel. *Tribology International*, 41(7):663–671, 2008. cited By 103.

[5] Maider Muro, Garikoitz Artola, Anton Gorriño, and Carlos Angulo. Wear and friction evaluation of different tool steels for hot stamping. *Advances in Materials Science and Engineering*, 2018:3296398, Mar 2018.

[6] S. Stupkiewicz and Z. Mróz. A model of third body abrasive friction and wear in hot metal forming. *Wear*, 231(1):124–138, 1999. cited By 43.

[7] J. Venema, J. Hazrati, D.T.A. Matthews, R.A. Stegeman, and A.H. van den Boogaard. The effects of temperature on friction and wear mechanisms during direct press hardening of al-si coated ultra-high strength steel. *Wear*, 406-407:149–155, 2018. cited By 36.

[8] J. Venema, D.T.A. Matthews, J. Hazrati, J. Wörmann, and A.H. van den Boogaard. Friction and wear mechanisms during hot stamping of alsi coated press hardening steel. *Wear*, 380-381:137–145, 2017.

[9] A. van Beek. *Advanced Engineering Design: Lifetime Performance and Reliability*. TU Delft, 2015.

[10] E. Gracia-Escosa, I. García, J.J.D. Damborenea, and A. Conde. Friction and wear behaviour of tool steels sliding against 22mnb5 steel. *Journal of Materials Research and Technology*, 6(3):241–250, 2017. cited By 33.

[11] Bernd-Arno Behrens, Anas Bouguecha, Milan Vucetic, and Alexander Chugreev. Advanced wear simulation for bulk metal forming processes. *MATEC Web of Conferences*, 80:04003, 01 2016.

[12] P.J. Blau. How common is the steady-state? the implications of wear transitions for materials selection and design. *Wear*, 332-333:1120–1128, 2015. cited By 54.

[13] X. Yuan, D. Zhou, D.J. Politis, G. Ma, and L. Wang. Tool life prediction under multi-cycle loading conditions: A feasibility study. volume 21, 2015. cited By 0.

[14] J. F. Archard. Contact and Rubbing of Flat Surfaces. *Journal of Applied Physics*, 24(8):981–988, 08 1953.

[15] K. Ersoy, G. Nuernberg, G. Herrmann, and H. Hoffmann. Advanced prediction of tool wear by taking the load history into consideration. volume 907, pages 697–702, 2007. cited By 1.

[16] Valentin Popov. Generalized archard law of wear based on rabinowicz criterion of wear particle formation. *Facta Universitatis, Series: Mechanical Engineering*, 17:39–45, 03 2019.

A Calibration current model

The model to determine Tool Wear (TW) that is currently implemented in TriboForm/AutoForm is an adaption of the Archard model [14], see Equation 18. In this model the real area of contact is multiplied with the wear rate and integrated over the sliding length of one stroke.

$$TW = \int k \cdot \alpha(P, \epsilon, T, \nu) dl \tag{18}$$

For this model an attempt was made to find a constant value for k, the wear rate. At 10 locations in the simulation and experimental data the tool wear value is collected. With this data the wear rate k can be determined, as follows from Equation 19 and 20.

$$TW = k \cdot model \tag{19}$$

$$k = \frac{TW}{model} \tag{20}$$

For the first 7 locations the wear rate is calculated with Equation 20. Something to note is that the experimental data shows the tool wear at the end of the lifetime, in this case after 170 000 strokes. The simulation shows the tool wear after 1 stroke. To be able to compare both the data sets, the experimental data is divided by the amount of strokes. The results are shown in Table 5.

Calibration				
	TW experimental data		TW simulation	k
Location	170 000 strokes	1 stroke	1 stroke	1 stroke
1	0.39	2.28758E-06	4.170	5.48581E-07
2	0.31	1.79939E-06	5.163	3.48128E-07
3	0.22	1.30719E-06	0.036	3.63108E-05
4	0.25	1.47059E-06	0.466	3.15577E-06
5	0.08	4.90196E-07	0.015	3.26797E-05
6	0.32	1.86275E-06	7.457	2.49798E-07
7	0.29	1.73203E-06	0.672	2.57742E-06
			Average	**1.08386E-05**

Table 5: Calibration of wear rate k

The average wear rate k was calculated from the data in Table 5. For the validation the tool wear in the experimental data is predicted with the average wear rate and the simulated tool wear value, as shown in Equation 19. The results are shown in Table 6.

Validation				
	Average k	TW simulation	TW experimental data	
Location			Prediction	Actual
8	1.08386E-05	0.00083	8.99604E-09	2.28758E-07
9	1.08386E-05	0.012	1.30063E-07	6.20915E-07
10	1.08386E-05	10.67	1.15648E-04	1.96078E-06

Table 6: Validation of wear rate k

As can be seen in the fourth and fifth column of Table 6, this did not give the desired result, since the prediction does not fall into the same order of magnitude as the actual tool wear value. This could have the following causes:

- The sample size is too small
- Inaccurate location comparison
- The wear rate is not a constant

- Incorrect model

The calibration had a sample size of 7 data points. This is, by all means, too small to draw any solid conclusions. However, the variance in the results do give an indication of the level of agreement between the simulation and experimental data, which did not give a good result. Another possible influence on the result is the way the locations are picked out. Since this is done manually, an error is introduced and the location comparison could be inaccurate. For this calibration it is assumed that the wear rate is a constant. However, it could be the case that the wear rate is dependent on a process parameter and therefore not constant. Another possibility is that the model is not correct. Since this model did not give the desired result, a closer look will be taken on the wear rate and the tool wear model to see if improvements can be made.

B Wear coefficients

Pressure model

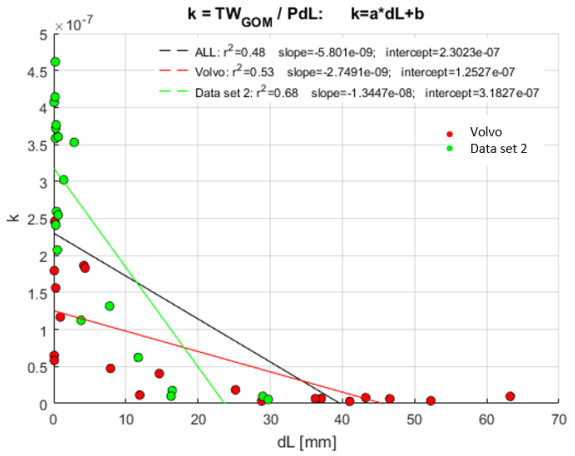

(a) Linear-linear

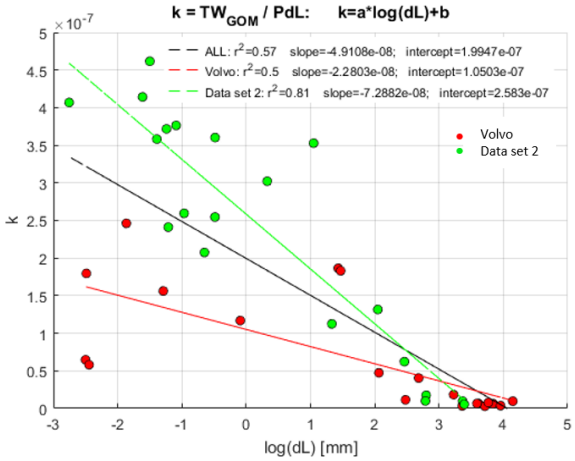

(b) Logarithmic-linear

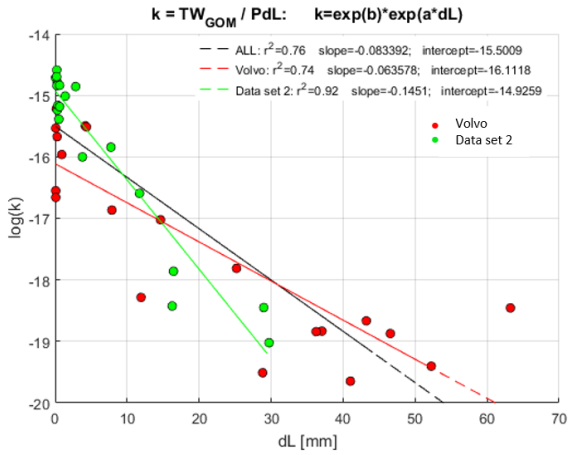

(c) Linear-logarithmic

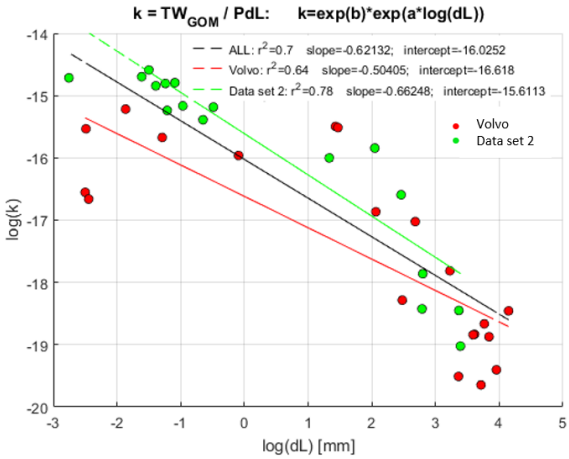

(d) Logarithmic-logarithmic

Figure 31: Wear rate vs. sliding length for the pressure model, different combinations of linear and logarithmic axis

Contact Area model

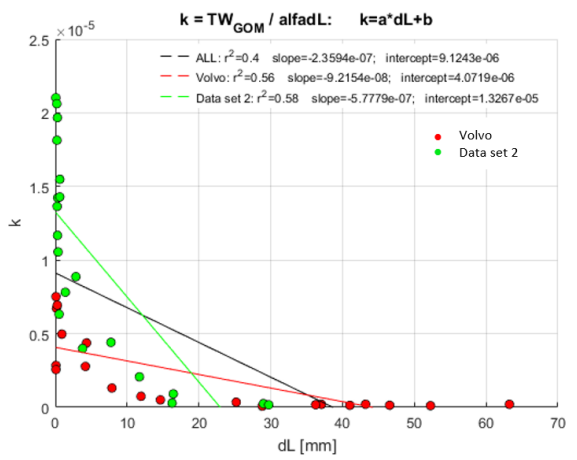

(a) Linear-linear

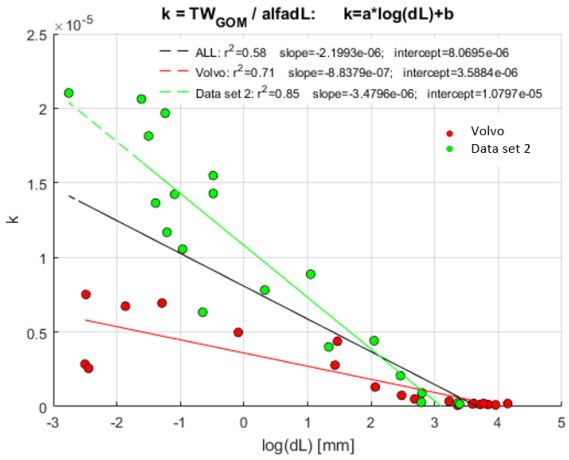

(b) Logarithmic-linear

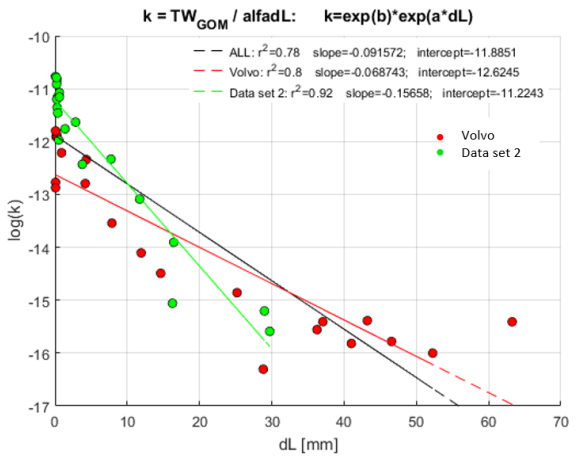

(c) Linear-logarithmic

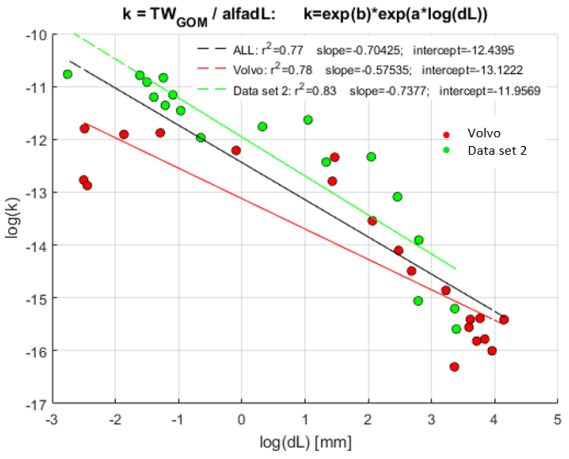

(d) Logarithmic-logarithmic

Figure 32: Wear rate vs. sliding length, different combinations of linear and logarithmic axis

C Simulation of the Contact Area

There are different ways to look at surfaces in contact. The nominal contact area is the area in contact on macro scale. However, at micro scale every surface has a roughness, which is built up from asperities. The real contact area only takes the actual contact between the tops of the asperities into account. When a large normal load is placed on the surfaces, the surface topography deforms and the asperities of the sheet are flattened. The deformation of the asperities is assumed to be plastic, so the asperities do not spring back once the load is removed. This means that the contact area cannot decrease during a forming process. The phenomena is called 'flattening'. The nominal and real contact area and flattening are illustrated in Figure 33.

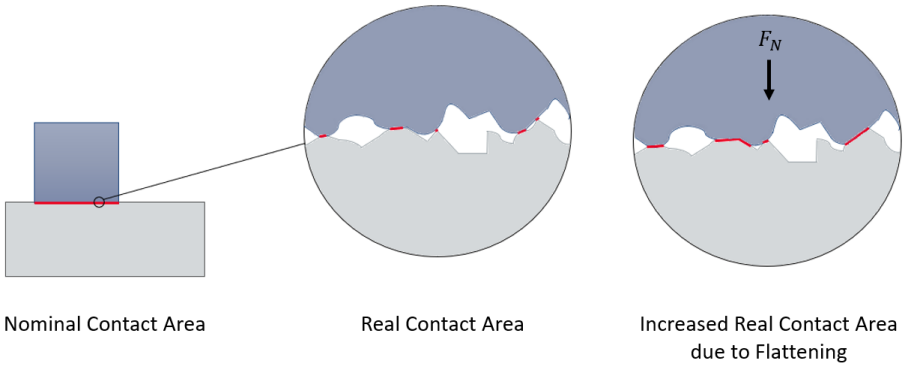

Figure 33: Contact Area and Flattening

With the material characteristics and the conditions at a specific location, i.e. the pressure, strain, temperature and velocity, it is possible to calculate the real contact area with the TriboForm software. The contact area is denoted with α and has a value between 0 and 1, where 0 means no contact and 1 indicates 100% contact. The contact area calculated with the conditions at that moment is called the incremental contact area. During a forming process the conditions change, and therefore the calculated contact area changes too. In Figure 34a this change in contact area during the forming process is shown for two locations. However, due to flattening the contact area cannot decrease during the forming process. Therefore, to simulate flattening the maximum contact area is used. With the maximum contact area the largest contact area that is experienced during the process is used for the consecutive steps. This is shown in Figure 34b. To analyse what physically happens to the surface topography the maximum contact area should be considered in forming simulations.

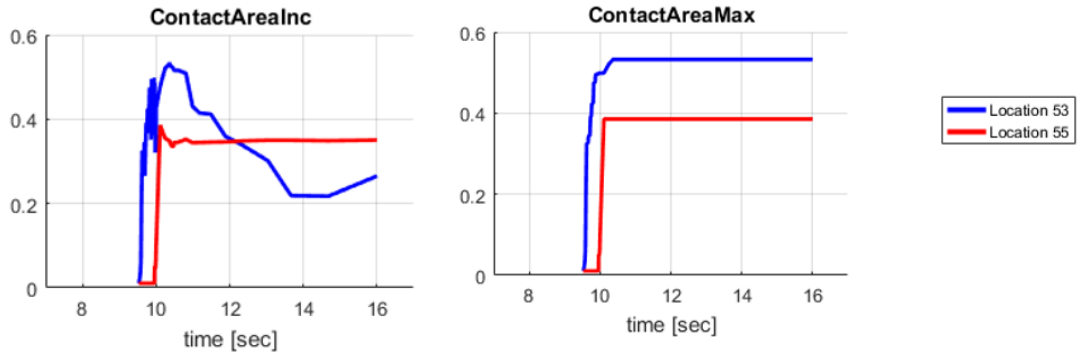

(a) Incremental Contact Area (b) Maximum Contact Area

Figure 34: Types Contact Area

To determine the maximum contact area, the sheet history is needed. In AutoForm this is available and the contact area is calculated in the post-processing step. It should be noted that the sheet history cannot be exported from AutoForm and can therefore not be used within this research. The only way

to include flattening of the sheet is to re-calculate the incremental contact area, based on the pressure, temperature, velocity and strain. The contact area of the tool is not relevant, as the tool is considered to be rigid and therefore does not deform.

To explain why it is inaccurate to calculate the contact area with the data currently available, a simplified situation is sketched in Figure 35. Location A and location B are indicated in the figure, with a yellow and red dot, respectively. These locations are used to explain the contact from the sheets perspective with location A and the tools perspective with location B. Figure 35b shows the start of the forming situation, the sheet moves along the tool until location A and B are in contact, as shown in Figure 35c.

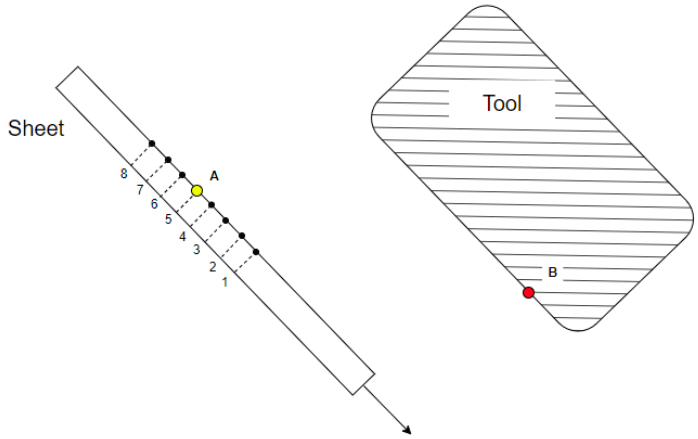

(a) Setup - separate sheet and tool

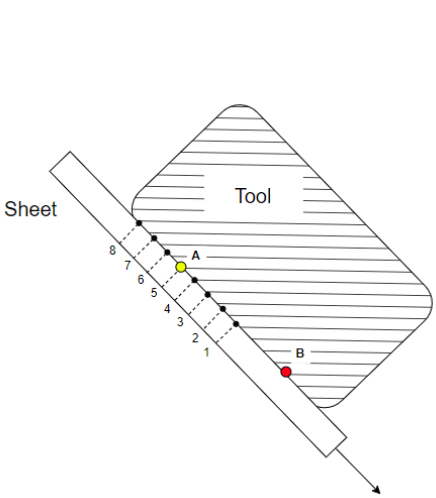

(b) Start position

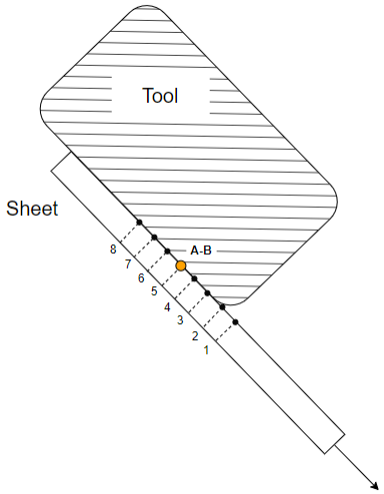

(c) A-B contact

Figure 35: Tool-sheet contact

In Figure 36 the incremental contact area is shown for the time steps from the situation in Figure 35b on. The incremental contact area is calculated with the conditions at every time step. The maximum contact area is plotted with the dashed line.

In Figure 36a the incremental contact area at location A, so from the sheets perspective, is shown. The time steps where location A is in contact with the tool are indicated with A1 to A8 in the graph. Note that the sheet experiences maximum flattening, α_{max}, at time step A4.

In Figure 36b the incremental contact area at location B, so from the tools perspective, is shown. The steps 1 to 8 in the graph correspond to the steps on the sheet in Figure 35. The step where location A

and B are in contact is indicated with an orange dot and subscript A-B in both graphs of Figure 36.

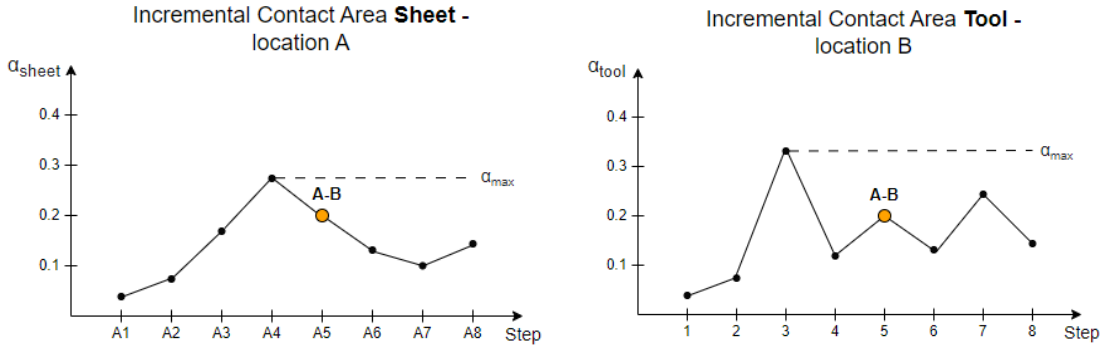

(a) Sheet perspective

(b) Tool perspective

Figure 36: Incremental Contact Area

The situation of the contact A-B from the sheets perspective in Figure 36a shows that the calculated contact area has a lower value than the sheet experienced in previous steps: $\alpha_{A-B} < \alpha_{maxA}$. To simulate the flattening correctly the α_{max}-value should be used. Unfortunately, the sheet history is not available in the data exported from AutoForm. This means that, for the current example, the calculated contact area is likely to be an underestimation of the actual contact area. This situation illustrates why the calculated contact area does not give an accurate representation from the sheets perspective.

In Figure 36b the contact area is plotted from the tools perspective. It is important to note that the sheet data is projected on the tool in AutoForm and that these conditions are used to calculate all parameters. At every step in this figure the tool is in contact with a new part of the sheet. The tool is assumed to be rigid and can, therefore, not deform. The sheet is made of a softer material and can deform. So any deformations that happen, only happen to the sheet. This means that the maximum contact area, the dashed line, from the tools perspective does not say anything. The tool did not deform and an increase in contact area is a result of deformation of the sheet, which is replaced by a new part of sheet in the next step. To make a correct calculation of the contact area, the sheet history is needed, but this is not available as mentioned before. This means that flattening cannot be taken into account and a correct value of the contact area cannot be calculated with this data.

From all this, it can be concluded that it is inaccurate to include flattening of the sheet and its resulting contact area as a parameter to model abrasive tool wear.